Analyzing Neurotransmitter-Receptor Signaling: An Information-Theoretic and Data-Driven Perspective

Amir Haeri

A Thesis Submitted to the Faculty of Graduate Studies
In Partial Fulfillment of the Requirements
for the Degree of Master of Science

Graduate Program in Computer Science

York University
Toronto, Ontario

July 2026

©Amir Haeri, 2026

Abstract

Neurotransmitter-receptor signaling is central to neuronal communication, but the information-transmission limits of different signaling systems remain unclear. This thesis studies neurotransmitter signaling using an information-theoretic framework in which neurotransmitter concentration is the channel input and receptor-state dynamics are the output.

Published kinetic models for serotonin, glutamate, GABA, and glycine signaling were represented as Markov models, and mutual information rate (MIR) was computed across concentration regimes and input probabilities. The results show that MIR is strongly shaped by receptor kinetics and concentration separation: increasing the ratio between the two input concentrations can improve information transmission, but the effect saturates or becomes non-monotonic when receptor responses are no longer well separated. Glutamate and glycine signaling produced the highest MIR in large concentration ratio regimes, while GABA signaling varied substantially across agonists and receptor models. The optimal input distribution often favored frequent low-concentration inputs and rare high-concentration inputs.

Acknowledgements

I would like to express my sincere gratitude to my supervisor, Professor Andrew Eckford, for his guidance, encouragement, and valuable feedback throughout my graduate studies. His support and belief in my work played an important role in shaping this thesis. I am also deeply grateful to my family for their constant love and support, especially during difficult times. Their care and resilience have been a source of strength throughout this journey.

I would like to thank my partner for her kindness, patience, and practical support. Her encouragement made a meaningful difference, especially during the most stressful stages of this process. Finally, I am thankful to my friends for being there for me with warmth and understanding. Their presence helped me stay grounded and reminded me that I was not alone.

Contents

Page

Abstract **ii**

Acknowledgements **iii**

Contents **iv**

List of Tables **vii**

List of Figures **viii**

1 Introduction **1**

1.1 Information theory and signaling systems 3

1.1.1 Signal Transduction and Channel Capacity 4

1.1.2 Information Processing in Biochemical and Living Systems 4

1.1.3 Theoretical Extensions 5

1.2 Information theory in neuroscience 6

1.2.1 Synaptic and Neuronal Information Processing 6

1.2.2 Information Theory in Cognitive Neuroscience 7

1.2.3 Applications of Information Theory 8

1.3 Other related works 10

1.4 Objectives 12

1.4.1 Implications 13

2 Biological and Mathematical Foundations **16**

2.1 Biological Background 16

2.1.1 Neurons, Synapses, and Neurotransmitters 16

2.1.2 The Input Signal: Neurotransmitter Concentration 19

2.1.3 Kinetics and Reaction Rates 20

2.2 Mathematical Background 22

2.2.1 Information Theory 22

2.2.2 Markov Chains 25
2.2.3 Hidden Markov Models 27

3 Information-Theoretic Analysis of Dopamine and Serotonin Signaling at the Human 5-HT$_{3A}$ Receptor 28

3.1 System model 29
3.1.1 Physical model 30
3.1.2 Mathematical model 32
3.2 Methodology 34
3.3 MIR Analysis 35
3.3.1 Effect of Input Probability p_L on MIR 36
3.3.2 Effect of the Concentration Ratio x_H/x_L on MIR 39
3.4 Discussion 43

4 Information-Theoretic Analysis of Fast Neurotransmitter Receptor Models 46

4.1 Motivation and Chapter Overview 46
4.2 Selection of Receptor Models 46
4.3 Glutamate Signaling via AMPA Receptors 47
4.3.1 Receptor Background and Kinetic Scheme 47
4.3.2 MIR Analysis 49
4.3.3 Results and Interpretation 50
4.4 GABA Signaling via GABA$_{\mathrm{A}}$ Receptors 52
4.4.1 Receptor Background and Agonists 52
4.4.2 Kinetic Scheme and Rate Constants 53
4.4.3 MIR Analysis 54
4.4.4 Results and Interpretation 56
4.5 Glycine Signaling via $\alpha_1\beta$ Receptors 57
4.5.1 Receptor Background and Kinetic Scheme 58
4.5.2 MIR Analysis 58
4.5.3 Results and Interpretation 60

4.6 Conclusion 61

5 Conclusion **64**

5.1 Main Findings 64

5.2 Limitations and Future Directions 66

5.3 Simplifications 67

5.4 Final Remarks 68

Bibliography **69**

List of Tables

2.1 A taxonomy summary of neurotransmitters and receptor mechanisms discussed in this thesis. Note that the following table classifies receptor mechanisms, not the neurotransmitter molecules themselves. A single neurotransmitter can act through different receptor families [1–5]. 19

3.1 Kinetic rate constants of 5-HT and DA at the human 5-HT_{3A} receptor derived from [6]. The parameter L_0 defines the equilibrium ratio between unliganded resting and open states $[R]/[O]$, but [6] do not provide explicit kinetic rates for the corresponding transition $R \leftrightarrow O$, instead treating L_0 as a thermodynamic constraint. We tested several plausible implementations of this transition and observed no significant change in the MIR. Therefore, we chose to omit the unliganded gating transition and ignore L_0 in the final model. 32

3.2 Peak MIR across concentration regimes. Concentrations are reported in μM and MIRs in bits/s. 39

3.3 Summary of controlled concentration ratio sweep for 5-HT and DA. 42

4.1 Rate constants for GluR1 and GluR4 channels, adapted from [7]. 48

4.2 Peak MIR across concentration regimes for GluR1 and GluR4 AMPA receptors. Concentrations are reported in μM and MIRs in bits/s. 50

4.3 Kinetic rate constants for transitions between states of $\alpha_1\beta_3\gamma_2$, $\alpha_4\beta_3\gamma_2$, and $\alpha_4\beta_3\delta$ $GABA_A$ receptors activated by GABA, muscimol, and THIP. Values are adapted from Mortensen et al. [8]. 55

4.4 Peak MIR values for the low-high concentration case in Figure 4.7. Values are reported in bits/s. 57

4.5 Kinetic rate constants for transitions scheme of the $\alpha_1\beta$ glycine receptor. Values are adapted from [9]. 60

4.6 Peak MIR summary for the $\alpha_1\beta$ glycine receptor across different glycine concentration regimes. 60

List of Figures

1.1 Conceptual analogy between neurotransmitter signaling and a computer communication system. The presynaptic cell, neurotransmitter, and postsynaptic cell are represented as the sender, message, and receiver, respectively. 2

2.1 A simplified conceptual representation of input-output processing, where neurotransmitter concentration $x(t)$ drives stochastic receptor-state dynamics and produces an observed receptor state $Y(t)$. 17

2.2 Simplified comparison of ionotropic and metabotropic neurotransmitter signaling adapted from [2]. (A) Ionotropic receptors couple neurotransmitter binding more directly to ion-channel activity, whereas (B) metabotropic receptors act through GPCR-mediated intracellular signaling before influencing the cellular responses. 20

2.3 Example conversion of receptor rate constants into state transitions and the corresponding generator matrix Q for a continuous-time Markov chain. Adapted from [10]. 26

3.1 Kinetic scheme for human 5-HT_{3A} receptor function, adapted from [6]. In each configuration, A is the ligand and A_kX ($k = 0, 1, 2, 3$ and $X \in \{R, O, D\}$) denotes a state with k ligand molecules bound. 31

3.2 MIR for (a) 5-HT and (b) DA at the human 5-HT_{3A} receptor for three concentration regimes based on [6]: sub-EC_{50} (concentrations below the half-maximal effective concentration (EC_{50})), near-EC_{50} (concentrations close to EC_{50}), and Solt experimental (exact concentrations reported in the study). The time step is dt = 0.002 ms. In all cases, the MIR is zero at $p_L = 0$ and $p_L = 1$, where the input is deterministic and the channel carries no information. For both plots, an inset subplot highlights the behavior near $p_L = 1$. 37

3.3 MIR for 5-HT and DA at the human 5-HT_{3A} receptor in the in vivo multi-region regime. The blue curve corresponds to DA and the orange curve to 5-HT. Concentration bounds are based on experimentally reported extracellular measurements across brain regions, capturing baseline and elevated activity levels: DA in [0.02, 0.2] μM [11, 12], and 5-HT in $[0.18 \times 10^{-3}, 68 \times 10^{-3}]$ μM [13]. 38

3.4 Peak MIR versus concentration ratio $c = x_H/x_L$ for the 5-HT_{3A} receptor model with fixed $x_L = 0.3$ μM. The MIR increases with c up to an intermediate optimum of 10.70 bits/s at $c \approx 840$ ($x_H \approx 252$ μM), then decreases and eventually converges to approximately 7.01 bits/s at large ratios. This non-monotonic trend shows that increasing the concentration contrast improves information transmission only up to an optimal range; beyond that, additional increases in x_H produce less distinguishable receptor dynamics and do not further improve MIR. 40

3.5 Peak MIR versus concentration ratio $c = x_H/x_L$ for DA at the 5-HT_{3A} receptor model with fixed $x_L = 30$ μM. The MIR rises steeply and saturates at $\approx$ 828 bits/s, retaining 94.3% of its peak value of 878 bits/s reached at $c \approx 455$ ($x_H \approx 13,700$ μM). 41

3.6 Optimal input probability p_L^* as a function of the concentration ratio $c = x_H/x_L$ for 5-HT and DA at the 5-HT_{3A} receptor model. For each value of c, p_L^* is the probability of the low concentration that maximizes the MIR. At small ratios, p_L^* is close to 0.5, indicating a nearly balanced optimal input distribution. As the ratio increases, p_L^* approaches one for both ligands, showing that the MIR is maximized when the low concentration is frequent and the high concentration is rare. 42

4.1 Kinetic transition scheme for the AMPA receptor, adapted from [7]. Low-probability gray states and transitions from the original model are excluded. 49

4.2 MIR as a function of p_L for (a) GluR1 and (b) GluR4 AMPA receptor models under different glutamate concentration ranges. Each curve compares a low concentration x_L with a high concentration x_H, using concentration pairs derived from the experimental results in [7]. 51
4.3 Kinetic transition scheme for $GABA_A$ receptor activation, adapted from [8]. The model includes agonist binding to resting closed states, transitions to mono-liganded and bi-liganded open states, and entry into a desensitized state. Here, A represents the agonist, R the receptor, AR^* and A_2R^* the open states, and A_2D the desensitized state. 54
4.4 MIR analysis for GABA at three $GABA_A$ receptor subtypes. The three subplots compare $\alpha_1\beta_3\gamma_2$, $\alpha_4\beta_3\gamma_2$, and $\alpha_4\beta_3\delta$. Each curve shows one concentration-pair case: low–mid, mid–high, or low–high. 55
4.5 MIR curves for muscimol across the three $GABA_A$ receptor subtypes. Each subplot corresponds to one receptor subtype, and each curve represents one concentration-pair case. 56
4.6 MIR curves for THIP across the three $GABA_A$ receptor subtypes. Each subplot corresponds to one receptor subtype, and each curve represents one concentration-pair case. 56
4.7 Comparison of MIR curves for GABA, muscimol, and THIP under the low-high concentration case. Each subplot shows one $GABA_A$ receptor subtype, and each curve represents the MIR as a function of the low-concentration input probability p_L. 57
4.8 Flipped-state kinetic scheme for glycine receptor activation adapted from [9]. Resting (R) states are shown in blue, flipped (F) states in red, and open (F^*) states in green. Horizontal transitions describe glycine binding and unbinding, while vertical transitions describe conformational changes between resting, flipped, and open states. 59
4.9 MIR analysis of the $\alpha1\beta$ glycine receptor model. The curves show the MIR as a function of the low-concentration input probability p_L for a binary glycine input with concentration levels x_L and x_H. 61

1 Introduction

In the human brain, neurons primarily communicate with each other through the release of chemical messengers known as neurotransmitters [14, 15]. These messages (neurotransmitters) are transmitted in small junctions in the brain called synapses. The presynaptic cell acts as the sender, and the postsynaptic cell acts as the receiver. Neurotransmitters trigger electrical responses in the postsynaptic cell by binding to a diverse class of proteins known as neurotransmitter receptors. Figure 1.1 shows a conceptual translation of synaptic communication into a communication-system framework. These receptors fall into two main categories: those in which the receptor itself functions as an ion channel, and those in which the receptor and ion channel are distinct molecules. The first type, known as ionotropic receptors or ligand-gated ion channels, generates rapid postsynaptic responses that typically last only a few milliseconds. The second type, called metabotropic receptors, produces slower postsynaptic effects that can persist for much longer durations. A detailed comparison between these two classes of receptors is provided in Section 2, Figure 2.2.

There are over 100 known neurotransmitters, giving the brain remarkable variety in how neurons communicate. Based on size, they fall into two main groups: neuropeptides, which are larger molecules made up of 3 to 36 amino acids, and small-molecule neurotransmitters, which include single amino acids like glutamate and GABA, as well as chemicals such as acetylcholine, serotonin, and histamine. Within the small-molecule group, a subset called biogenic amines, including dopamine, norepinephrine, epinephrine, serotonin, and histamine, share similar chemical structures and produce comparable effects on their target cells [14].

Because neurotransmission involves a signal, a receptor, and a measurable response, it can also be viewed as a biological communication process. In this view, the neurotransmitter concentration acts as the input signal, while the receptor state or downstream cellular response acts as the output. This creates a natural connection between neuroscience and information theory, since both are concerned with how reliably a message can be transmitted through a noisy system.

In 1948, Claude Shannon stated that "the fundamental problem of communication is that of reproducing at one point either exactly or approximately a message selected at another

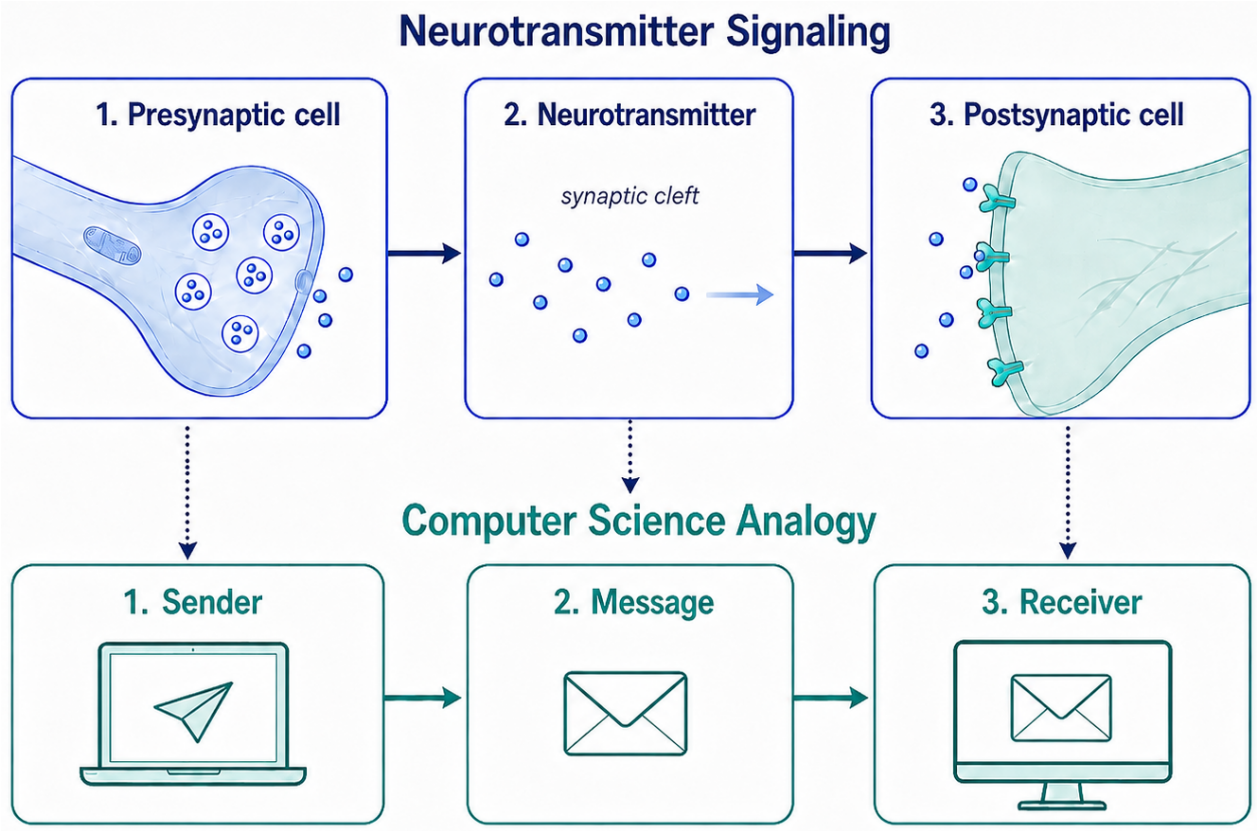

Figure 1.1: Conceptual analogy between neurotransmitter signaling and a computer communication system. The presynaptic cell, neurotransmitter, and postsynaptic cell are represented as the sender, message, and receiver, respectively.

point." In this thesis, this idea is interpreted in terms of a biological signaling channel, where the original message corresponds to the input signal and the reproduced or observed effect corresponds to the output response. Mutual information provides a way to quantify this relationship by measuring how much observing the output reduces uncertainty about the input message. In other words, it quantifies how much information the response carries about the original signal [16]. If the input is represented by the random variable X and the output response by the random variable Y, their mutual information is given by

$$I(X;Y) = \sum_x \sum_y p(x,y) \log \frac{p(x,y)}{p(x)p(y)},$$

where $p(x,y)$ is the joint probability of the input and output, and $p(x)$ and $p(y)$ are their marginal probabilities [17]. Another related concept in information theory is the capacity of a channel. The maximum possible information that a channel can carry, called the channel

capacity, is

$$C = \sup_{p_X(x)} I(X;Y).$$

In the above formula, the supremum is evaluated over all possible choices of the input probability distribution. Capacity is an inherent feature of the channel: the larger the value, the more information the channel can theoretically transmit [17].

One might ask why information theory should be used in neuroscience and biological communication channels. A concise answer is provided in [18]: information theory is valuable in neuroscience because it is model independent, allowing relationships within data to be quantified without assuming a specific underlying model. It works with different types of data, including continuous, discrete, raw, or processed data, and can detect both linear and nonlinear interactions, which are common in neural systems. It is also naturally multivariate, making it well-suited for modern neuroscience techniques that record many variables simultaneously.

Another strength of information theory is that results are expressed in bits, enabling direct comparisons across experiments, brain regions, and subjects. These strengths make information theory particularly powerful for analyzing complex neural systems, despite certain limitations. Similarly, [19] explains that Shannon's information theory provides a mathematical framework that is independent of network complexity and can quantify how much information can be transmitted despite biochemical noise. With information theory, a complex biological system can therefore be reduced to a black-box communication channel and analyzed in terms of its input-output relationship.

1.1 Information theory and signaling systems

Information theory provides a rigorous framework for quantifying how signals are generated, transmitted, and decoded [20]. In living organisms, molecular and cellular processes can be viewed as channels that convey information through chemical, electrical, or mechanical means. Understanding these processes from an information-theoretic perspective allows researchers to measure the efficiency, fidelity, and limitations of biological communication,

bridging concepts from Shannon's theory with biochemical and neural signaling.

This section explores how information theory models the mechanisms of signal transduction, quantifies information flow in biochemical systems, and extends to theoretical frameworks that describe the meaning and optimization of information in living systems.

1.1.1 Signal Transduction and Channel Capacity

In [21], the authors explain that the intersection of biology and information theory comes from the convergence of two fields. In the first one, quantitative biologists apply information-theoretic analysis to interpret laboratory data. In the second one, information theorists explore biological applications of information theory, broadly to the advantage of molecular biology and neuroscience. These two areas have also supported the development of biologically inspired communication systems.

In particular, **(author?)** [10] describe signal transduction as a communication system where the receiver is the signal transduction receptor, modeled as a finite-state Markov chain with transition rates controlled by the input signal. Signal transduction can have many forms, and the input signal can include changes in chemical concentration, electrical potential, light intensity, mechanical force, temperature, and other quantities.

In their results, an explicit formula is given for the mutual information under independent and identically distributed inputs. Conditions under which the formula gives the channel capacity are also provided, specifically when there exists exactly one transition in the Markov chain that is sensitive to the channel input. This result is then used to find the channel capacity of Channelrhodopsin-2 and other biological receptors.

1.1.2 Information Processing in Biochemical and Living Systems

Biochemical noise and its implications are central to **(author?)** [17], who show that biochemical noise can drastically lower the fidelity of signaling. This raises the question of how networks that control cell-fate decisions can function reliably under such noise.

Life revolves around information. The central dogma, from DNA to mRNA to protein, shows how genetic information flows, while organisms also process environmental information

to survive and adapt. Information therefore explains both biological processes and evolutionary outcomes [22].

Roughly speaking, biochemical information processing includes sensing or detecting input signals, transmitting or recovering those signals, storing cellular memory, and integrating relevant information to drive reliable responses. In [23], the authors propose that, despite the complexity and apparent disorder of evolved biological systems, it is possible to develop a predictive theoretical framework by integrating concepts from chemical kinetics, information theory, decision-making, and evolutionary optimization. They also review the optimization of information, which suggests that biological systems may have evolved to optimize the gathering and representation of information.

Signaling networks are biochemical systems that process information about the environment through extracellular stimuli. Noise in such systems maps one input to many possible output responses, resulting in a loss of information about the input [24]. In the same study, the authors developed a framework to predict and measure the mutual information transduced by one or more signaling pathways. Their study shows that molecular noise strongly limits how much information a single cell can process.

According to **(author?)** [19], within a recipient cell, the information inside a chemical message must be captured and processed by the cell's biochemical circuitry. This process involves feedback loops, crosstalk, and delays. In this structure, molecular noise can strongly impede the propagation of signals. Using information theory, one can reduce a complex system to a black-box communication channel and analyze it. They show how information theory helps analyze biological signaling by using channel capacity to measure information flow and rate-distortion theory to study error-performance tradeoffs. Its strength lies in offering insights into what signaling systems can or cannot achieve, even without detailed knowledge of all internal complexity. This conclusion ties back to the earlier themes of noise and optimization in biological information processing.

1.1.3 Theoretical Extensions

The notion of semantic information is central to **(author?)** [25], who define it as the portion of syntactic information a physical system holds about its environment that is required for the

system to maintain its own existence. The key questions are whether semantic information can be formally defined in a general way, and whether such a definition can apply to all physical systems, not only living ones.

Their results define semantic information based on a system's own dynamics with its environment, combining insights from information theory and non-equilibrium physics. Their framework separates information into meaningful and meaningless bits and offers a quantitative way to capture related ideas such as the value of information, semantic content, and agency. Unlike syntactic information, such as mutual information, semantic information can potentially misrepresent the world and is also asymmetrical. Lastly, it is suggested that having high levels of semantic information is necessary, but not sufficient, for any physical system to be alive.

1.2 Information theory in neuroscience

Information theory has become a fundamental framework for understanding how the brain encodes, transmits, and transforms information. It now provides quantitative tools to study how neurons and networks process sensory inputs, generate spikes, and support cognition. By treating neural activity as a communication channel, researchers can estimate how much information is conveyed about stimuli, how efficiently it is transmitted, and how noise, redundancy, and energy constraints shape neural coding strategies [10, 18, 26].

1.2.1 Synaptic and Neuronal Information Processing

If we have a neuron called j, then neuron j receives many inputs, converts them into a spike pattern, and sends that pattern forward. This is the essence of how neurons communicate [27]. Neurons can be viewed as nano-machines that use electrochemical signals and molecular communication to send information [28].

(author?) [28] highlight that electromagnetic-based communication is infeasible at nano-size dimensions, making molecular communication essential. This paradigm has three parts: axonal pathway, synaptic transmission, and spike generation, with the axonal pathway being the main issue investigated in their study. The paper models axonal input as a doubly Poisson spike train with Poisson-distributed noise and analyzes its impact on channel capacity.

Information-theoretic analysis also extends to synapses. **(author?)** [29] point out that Shannon's information theory is powerful because it can be used to study any kind of communication, including communication in the brain. While most previous work focused on single neurons, their study focuses on synapses to estimate how much information is transferred from one neuron to the next. By using tools such as mutual information and channel capacity, they aim to find the upper limits of how effectively synapses, both bipartite and tripartite, can pass on information. They show that synapses can only carry a limited amount of information, often only a few tenths of a bit per second.

Similarly, **(author?)** [30] note that the application of information theory in the analysis of synapses has received little attention, even though synapses exhibit sparse connectivity, noise, and widely distributed synaptic weights. Their study looks at how synapses store information under resource constraints. Boosting the signal-to-noise ratio can improve storage capacity, but it requires larger synaptic weights, which in turn require more volume. Since volume is costly, the main challenge is to maximize information storage under these constraints.

1.2.2 Information Theory in Cognitive Neuroscience

(author?) [31] provide a well-structured introduction to information theory in neuroscience. They describe feedback and why it matters, information theory and communication, and intra-organism communication. Information theory provides a way to measure information and understand the limits of compression and communication. In addition, a common information-theoretic method in computational neuroscience is to estimate the mutual information between observed sets of data.

The authors proposed a biologically grounded neuron channel model and calculated its channel capacity, showing that it is maximized using a discrete distribution. These concepts directly connect to the need for realistic models of how neurons communicate through spikes, since neuro-spike communication uses neurotransmitters as information carriers and remains largely unexplored [32].

Molecular communication is a paradigm that can be used in nanonetworks. Nanonetworks are the interconnections of nanomachines or nano-sized robots. In this context, molecular communication treats molecules, such as calcium ions and neurotransmitters, as information

carriers. Among these paradigms, neuro-spike communication stands out as being largely unexplored.

In neuro-spike communication, neurotransmitters are the information carriers, and the performance of this communication is described as strong in terms of reliability, speed, and robustness. In [32], the neuro-spike channel between one input neuron and one output neuron in the CA region is analyzed. The study finds that neuro-spike communication is more reliable with low input rates, more NMDA receptors, and less noise. These factors may relate to brain disorders, and the model could also inspire future nanoscale networks.

The free-energy principle is a theory for learning and memory which predicts that neurons, synapses, and neuromodulators work in a way that minimizes free energy. Neuromodulation through dopamine and noradrenaline is very important for processing information in the brain. For example, the death of dopamine neurons causes Parkinson's disease, while abnormal regulation of their activity is associated with schizophrenia [33].

Using theoretical analysis and numerical simulations, **(author?)** [33] characterize the effect of changing dopamine and noradrenaline concentrations on the recovery of the first principal component. Their scheme can be applied in computational psychiatry to model dysfunctional neural networks underlying positive symptoms of schizophrenia, linked to abnormal dopamine levels, and to capture the role of noradrenaline in memory prioritization and posttraumatic stress disorder. These insights expand the scope of information-theoretic and molecular communication frameworks by linking communication efficiency and robustness to neuromodulation and psychiatric conditions.

1.2.3 Applications of Information Theory

(author?) [34] first discuss the main role of information theory in neural coding. They mention that information theory quantifies how much information a neural response carries about a stimulus. The term "neural code" refers to the neural representation of information. Studying neural codes asks what is being encoded, how it is encoded, and with what precision. Here, information theory can be used to quantify the reliability and usefulness of stimulus-response functions.

The authors find that simple models capture much of the information neurons transmit,

with each spike adding to coding efficiency. Spike timing is precise, but mainly just enough to represent the stimulus, rather than creating a separate temporal code. These principles also support advances in applying molecular communication and nanotechnology to brain-machine interfaces and neural disorders [35, 36].

(author?) [35] discuss brain disorders that disrupt synaptic communication and explore how advances in molecular communication research could lead to brain implant technologies. They focus on understanding synaptic processes to design biomimetic brain-machine interfaces for diagnosing and treating brain diseases. Three classes of brain-machine interfaces exist: sensory, motor, and cognitive.

The main finding of **(author?)** [35] is that advances in molecular communication and bio-nanotechnology are paving the way for synaptically interactive brain-machine interfaces that can mimic and regulate neural pathways. However, significant open challenges remain before these systems can be applied clinically. Extending these ideas, **(author?)** [36] highlight that micro- and nano-scale devices connected to neurons can create neural-like nanonetworks, which may provide new directions for the diagnosis and treatment of neural disorders.

(author?) [36] show that Shannon's information theory can be used to quantify the amount of information exchanged between neurons. Their contributions include advancements in single-synaptic channel modeling, extension to multiple-access synaptic channels, and a mathematical method that could potentially serve as a core module of future cognitive brain-machine interfaces. They also propose a bottom-up approach that begins with computations of information rates in individual synapses, then extends to multiple synapses, multiple neurons, and eventually the brain.

In parallel, **(author?)** [37] discuss Alzheimer's disease and how it enables the exploration of information as a physical process central to brain disease progression. Neuronal loss and brain shrinkage from protein misfolding impair core cognitive functions, indicating disrupted neural information processing. Overactive microglia can also cause immune imbalance and inflammation, reflecting disordered immune information processing. These insights strengthen the case for considering molecular communication and information-carrying molecules as central to both disease mechanisms and therapeutic design.

In molecular communication, molecules are used as information carriers for communica-

tion between objects. This has several advantages over traditional electromagnetic-wave-based communication: molecule-based systems are biocompatible, operable in challenging environments, and energetically efficient. They also have a wide range of applications, such as the Internet of Bio-Nano Things, targeted drug delivery, and agricultural monitoring.

(author?) [38] review the role of information-carrying molecules and their properties, which are often disregarded in molecular communication studies. The authors show that these molecules play a critical role and should not be overlooked. They argue that recognizing their unique properties is essential for moving from theory to practice. By providing a comprehensive overview, the survey offers researchers a foundation for future studies that integrate molecular characteristics into models, experiments, and real-world applications.

1.3 Other related works

Recently, the study of psychedelic drugs has provided an opportunity to study the relationship between the mind and brain, as well as to improve mental health treatments. Although some of their chemical effects are known, it is still not fully understood how they work across the whole brain. Learning this could deepen our knowledge of consciousness and improve therapies. On the brain level, two major patterns stand out: reduced alpha brainwave activity, around 8–12 Hz, and increased complexity or diversity of brain signals, often described using the concept of entropy [39].

Research in both humans and animals shows that psychedelics produce their effects mainly by activating the serotonin 2A receptor. Building on this information-theoretic perspective, **(author?)** [40] used tools such as Shannon entropy, mutual information, and noise correlation across neuron pairs to examine how serotonin bioavailability affects medial prefrontal cortex coding of conditioned stimuli. This approach avoids assumptions about the neural code and has been widely applied to study population coding, neural interactions, and information redundancy or synergy. The authors concluded that with long-term Prozac treatment, the prefrontal cortex processes reward signals in a way that carries more information, but those signals become less stable and more vulnerable to noise.

Extending the role of information-theoretic measures from neurotransmitters to synaptic mechanisms, Santiago Ramón y Cajal suggested in 1894 that memories are stored in

synapses rather than by creating new neurons. Shannon information theory was later used to measure synaptic information storage capacity by calculating the bits stored in synaptic strengths. Information storage efficiency was assessed by comparing synaptic strength distributions, obtained from spine head volumes, with the maximum entropy distribution, showing near-maximal efficiency. These measures can also evaluate how factors such as pre- and postsynaptic features or brain-region differences affect synaptic information storage capacity [41].

Such findings resonate with the broader effects of psychoactive drugs on dopamine and serotonin systems. All drugs of abuse boost dopamine signaling in the limbic system. Alcohol does this by increasing dopamine cell firing, while psychostimulants block dopamine reuptake. This spike-driven release is known as the phasic dopamine response and underlies rewarding effects. On the other hand, extracellular dopamine is thought to be regulated by cortico-accumbens inputs, creating a steady-state signal known as the tonic dopamine response. **(author?)** [42] examine how psychostimulants and ethanol alter the dopamine system and how these changes can lead to addiction and craving.

In parallel to these brain-focused studies, molecular communication research offers a complementary framework for understanding how information can be transmitted through biological and nanoscale systems. Molecular communication lets tiny devices share information, which is useful for nanoscale Internet-of-Things applications and medical tasks such as drug delivery or disease detection. It uses molecules to carry signals, but because they spread slowly, signals can overlap and cause intersymbol interference.

(author?) [43] proposed a deep learning-based receiver that considers diffusion effects, counting noise, and intersymbol interference, showing improved performance over traditional methods in simulations. Their analysis also examined the impact of factors such as diffusion rate, distance, modulation, frame duration, and robustness to channel mismatches.

Building on this, nanoscale communication is attracting growing attention for its ability to link nanomachines into nanonetworks, especially inside the human body. Molecular communication is particularly promising because it works naturally at the nanoscale and is biocompatible. In molecular communication-based targeted drug delivery systems, nanodevices release drug molecules directly to infected tissue. However, because diffusion is

random, some molecules miss their target, which reduces treatment effectiveness and causes side effects [44].

1.4 Objectives

The objective of this thesis is to calculate the information-transmission ability of biologically important neurotransmitter receptor systems. In particular, this work analyzed serotonin and dopamine acting through the human 5-HT_{3A} receptor, glutamate acting through AMPA receptor models, GABA acting through $GABA_A$ receptor models, and glycine acting through a glycine receptor model. For these systems, we used published kinetic receptor models and computed **mutual information rates (MIRs)** under different neurotransmitter concentration conditions. Our study quantified MIRs for multiple neurotransmitter receptor systems and provided a quantitative framework that connects molecular-level signaling with information transmission. By defining information-theoretic baselines for neurotransmission, this work can help neuroscientists and pharmacologists evaluate how efficiently neural receptors transmit information under different signaling conditions.

(author?) [45] explain that a kinetic model for dopamine is a system of differential equations that mathematically describes dopamine release, diffusion, and reuptake, thereby predicting the temporal dynamics of extracellular dopamine concentrations. A similar idea can be extended to other neurotransmitters, where kinetic models aim to capture the binding, unbinding, gating, desensitization, and recovery dynamics of receptor-mediated neurotransmission. In this thesis, we used existing kinetic models from prior experimental and theoretical studies to connect receptor dynamics with information-theoretic analysis.

Biological receptors can be modeled as finite-state Markov chains whose states represent receptor conformations, such as closed, open, or desensitized. The receptor dynamics can be described by a master equation with an input-dependent transition-rate matrix, $Q(x(t))$. By discretizing the continuous-time model as $P = \exp(Q\Delta t)$, the receptor can be interpreted as a communication channel, where the input is the stimulus concentration and the output is the receptor-state sequence. This framework shows that input-sensitive transitions are the main source of information transmission [10, 46, 47].

Experimental and kinetic studies of neurotransmitter receptors commonly describe recep-

tor behavior using state-transition models whose parameters are estimated from measured response data. These models capture key biochemical processes such as ligand binding and unbinding, channel opening and closing, desensitization, and recovery. Differences in these transition rates determine how receptors respond to changes in neurotransmitter concentration and therefore shape the temporal dynamics of the observed receptor-state sequence [48, 49].

By combining kinetic state-transition models with information-theoretic channel analysis, our study computed MIRs for several neurotransmitter receptor systems. The analysis included concentration-dependent comparisons, input-probability optimization, receptor-specific kinetic effects, and the contribution of receptor dynamics to information throughput.

1.4.1 Implications

(author?) [37] demonstrated that soluble amyloid-beta oligomers disrupt synaptic transmission by impairing both presynaptic and postsynaptic signaling, leading to neuronal communication failures characteristic of informational disorders. Such disruptions highlight how noise introduces uncertainty in signal transmission. Mutual information, in this context, quantifies how many distinct input signals, such as ligand concentrations, can still be accurately differentiated despite inherent noise [24].

Dysregulation of dopamine and serotonin systems is implicated in a range of neurological and psychiatric disorders, including Parkinson's disease, schizophrenia, depression, and addiction [33, 42]. Quantifying the information-transmission ability of receptor signaling could clarify how reduced transmission fidelity or increased receptor noise contributes to cognitive and behavioral symptoms.

Beyond neuroscience, the same framework extends to biomedical engineering domains such as targeted drug delivery, where uncertainties in injection, nanoparticle transport, and receptor binding collectively influence the system's mutual information and bioequivalence. An information-theoretic perspective therefore offers useful insight into the reliability and efficiency of drug delivery pathways [50].

Moreover, understanding receptor-level information processing could inspire advances in biomimetic molecular communication systems, nanoscale biosensors, and medical nanoma-

chine architectures [35, 36, 51]. Finally, models that link biochemical kinetics to information throughput may guide the design of synthetic receptors or nanoscale biosensors optimized for signal fidelity [38, 43].

This thesis extends the information-theoretic analysis of biological signal transduction to the study of biologically important neurotransmitter receptor systems. While previous work has modeled signal transduction receptors as communication channels and derived capacity results for intensity-driven receptors such as Channelrhodopsin-2 [10], similar analyses have not been systematically applied across neurotransmitter receptor systems.

In this work, we combined the communication-channel framework of receptor signaling with experimentally derived kinetic models of the human 5-HT_{3A} receptor, AMPA receptors, $GABA_A$ receptors, and glycine receptors. Using these kinetic models, we computed MIRs and related information-theoretic metrics to characterize neurotransmitter signaling.

Our contributions include a systematic comparison of neurotransmitter signaling from an information-theoretic perspective, the analysis of information transmission as a function of neurotransmitter concentration, and the study of how receptor dynamics influence information throughput. We also investigated how input concentration ranges and input probabilities affect peak MIR, and how different kinetic receptor mechanisms produce different information-transmission patterns. Finally, we analyzed how receptor Markov models contribute to overall information transfer, providing insight into which biochemical mechanisms most strongly affect signaling fidelity.

The remainder of this thesis is organized as follows. **Chapter 2** presents the biological and mathematical foundations needed for the analysis. It introduces the main neurotransmitter and receptor concepts used in this work, explains how neurotransmitter concentration can be interpreted as an input signal, and describes the kinetic and Markov-chain framework used to model receptor-state dynamics. It also introduces the information-theoretic concepts used throughout the thesis, including mutual information and MIR.

Chapter 3 applies this framework to serotonin and dopamine signaling at the human 5-HT_{3A} receptor. It presents the receptor model, describes the construction of the transition-rate matrix, and analyzes how MIR changes across different concentration regimes, concentration ratios, and input probabilities.

Chapter 4 extends the same information-theoretic analysis to additional neurotransmitter receptor models, including glutamate AMPA receptors, $GABA_A$ receptors, and glycine $\alpha_1\beta$ receptors. This chapter compares MIR across receptor models, receptor subtypes, agonists, and concentration conditions in order to examine how receptor kinetics shape information transmission.

Finally, **Chapter 5** concludes the thesis by summarizing the main findings, discussing the limitations of the study, and outlining possible directions for future research.

2 Biological and Mathematical Foundations

This chapter introduces the biological, mathematical, and information-theoretic concepts used throughout this thesis. The main goal of this chapter is to provide the theoretical and biological foundations needed to model neurotransmitter receptors as stochastic communication systems, while keeping the discussion accessible to a computer science audience. In this view, an extracellular neurotransmitter concentration acts as the input signal, receptor state transitions form the channel dynamics, and receptor activation or opening represents the observable output. This framework allows biological signaling to be studied not only in terms of biochemical response, but also in terms of how much information about the input can be transmitted through receptor dynamics.

The chapter is organized as follows. Section 2.1 introduces the biological background needed for this thesis, beginning with neurons, synapses, and neurotransmitters. It then explains how neurotransmitter concentration can be interpreted as the input signal and how receptor kinetics and reaction rates describe receptor-level behavior. Section 2.2 presents the mathematical background, including the information-theoretic tools used in this work and the Markov chain framework used to model stochastic receptor state transitions.

2.1 Biological Background

This section introduces some biological and neurological terminology and concepts needed to understand the receptor models studied in this thesis. Since the intended audience includes computer science readers, the emphasis is on explaining the main biological components in simple computational terms. The main idea is that neurotransmitter signaling can be interpreted as an input-output processing channel: a chemical signal is released (the neurotransmitter), receptors detect this signal, and the receptor response changes the state of the cell (Figure 2.1).

2.1.1 Neurons, Synapses, and Neurotransmitters

Neurons communicate with each other through specialized junctions called synapses. In a chemical synapse, the presynaptic neuron (sender of the messages) releases chemical mes-

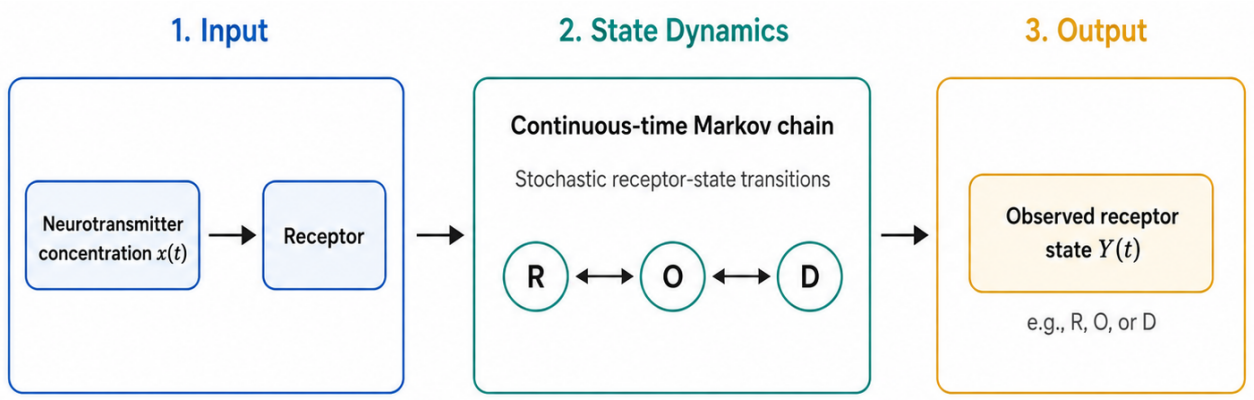

Figure 2.1: A simplified conceptual representation of input-output processing, where neurotransmitter concentration $x(t)$ drives stochastic receptor-state dynamics and produces an observed receptor state $Y(t)$.

sengers called neurotransmitters into the synaptic cleft, which is the small space between the presynaptic and postsynaptic cells (receiver of the messages). These neurotransmitter molecules are released across the cleft and bind to receptors located on the postsynaptic membrane. The receptor response then converts the chemical signal into an electrical or biochemical response in the postsynaptic cell [52].

From a communication perspective, the neurotransmitter can be viewed as the transmitted signal. The presynaptic neuron controls the release of the signal, the synaptic cleft acts as the transmission space, and the postsynaptic receptor system acts as the receiver. However, this process is not perfectly deterministic. Neurotransmitter release, diffusion, binding, and receptor activation all involve stochastic molecular events [22, 53].

Neurotransmitters include molecules such as glutamate, GABA, glycine, dopamine, and serotonin. These molecules differ in their chemical structure, receptor targets, and functional roles. Importantly, a neurotransmitter is not classified only by the molecule itself, but also by the receptor through which it signals. In this literature, the phrase *neurotransmitter signaling through a receptor* means that a neurotransmitter molecule binds to a specific receptor protein and produces a cellular response through that receptor. For example, glutamate signaling through AMPA receptors means that glutamate binds to AMPA receptors, which can open an ion channel and allow ions to flow across the postsynaptic membrane [7]. There are two major receptor-level mechanisms of neurotransmitter signaling [2].

- **Ionotropic signaling:** the neurotransmitter binds to a ligand-gated ion channel. In this case, the receptor itself contains an ion-channel pore. Binding of the neurotransmitter can open or close the channel, allowing ions such as Na^+, K^+, Ca^{2+}, or Cl^- to flow through the membrane. This mechanism is usually fast and is commonly associated with rapid synaptic transmission.

- **Metabotropic or GPCR signaling:** the neurotransmitter binds to a G protein-coupled receptor (GPCR). In this case, the receptor does not directly form an ion channel. Instead, receptor activation triggers intracellular signaling pathways through G proteins and second messengers. This mechanism is usually slower than ionotropic signaling, but it can produce longer-lasting and more modulatory effects.

In this context, the word *type* can refer to different levels of biological organization. A neurotransmitter type refers to the chemical messenger, such as glutamate, GABA, glycine, serotonin, or dopamine. A receptor type refers to the protein family that detects that specific neurotransmitter, such as AMPA, $GABA_A$, glycine, 5-HT_3, or dopamine receptors. A receptor subtype refers to a more specific version of a receptor, often defined by subunit composition or gene family. For example, $GABA_A$ is a receptor type, while $\alpha 1 \beta 3 \gamma 2$ is a receptor subtype or subunit composition [8]. Therefore, when we say that a neurotransmitter signals through a particular receptor, it means that the neurotransmitter binds to that receptor and that the receptor's state transitions determine the resulting cellular response.

Table 2.1 provides a brief taxonomy of the mentioned neurotransmitters and the group they belong to, as well as the ones that we focus on in this thesis.

This thesis mainly focuses on ionotropic receptors because they have relatively direct input-output dynamics. A neurotransmitter binds, the receptor changes state, and an ion channel may open. This makes them suitable for modeling with kinetic schemes and continuous-time Markov chains. However, GPCRs are also important for future extensions because they represent a more complex form of biochemical communication.

Table 2.1: A taxonomy summary of neurotransmitters and receptor mechanisms discussed in this thesis. Note that the following table classifies receptor mechanisms, not the neurotransmitter molecules themselves. A single neurotransmitter can act through different receptor families [1–5].

Neurotransmitter	**Ionotropic Receptors**	**GPCR Receptors**	**Our Focus**
Serotonin (5-HT)	5-HT_3	5-HT_1, 5-HT_2, 5-HT_4–5-HT_7	5-HT_3 receptors
Dopamine (DA)	None	D_1-D_5	Dopamine effects on the human 5-HT_{3A} receptor model
Glutamate (Glu)	AMPA, NMDA, kainate	mGluR1-mGluR8	AMPA receptors
GABA	$GABA_A$	$GABA_B$	$GABA_A$ receptors
Glycine (Gly)	GlyR	None	GlyR receptors

2.1.2 The Input Signal: Neurotransmitter Concentration

The main input variable in this thesis is neurotransmitter concentration. Concentration describes how much neurotransmitter is present in a given space. In synaptic signaling, the most relevant space is often the extracellular region around the receptor, especially the synaptic cleft. After release, neurotransmitter molecules diffuse through this extracellular space, bind to receptors, and are eventually removed by uptake, diffusion, or enzymatic degradation. Synaptic neurotransmitter concentration is not constant. It can vary depending on the amount of neurotransmitter released, the geometry of the synaptic cleft, diffusion, uptake mechanisms, and receptor location. In this thesis, concentration is simplified into discrete input levels. Most simulations use a binary input:

$$X \in \{x_L, x_H\}, \tag{1}$$

where x_L is a low neurotransmitter concentration and x_H is a high neurotransmitter concentration. The probability of the low-concentration input is denoted by p_L, and the probability of the high-concentration input is $1 - p_L$.

This binary simplification does not mean that real biological concentrations are only low or high. Rather, it provides a controlled way to ask how well a receptor can distinguish between two concentration conditions. If the receptor dynamics are very different under x_L

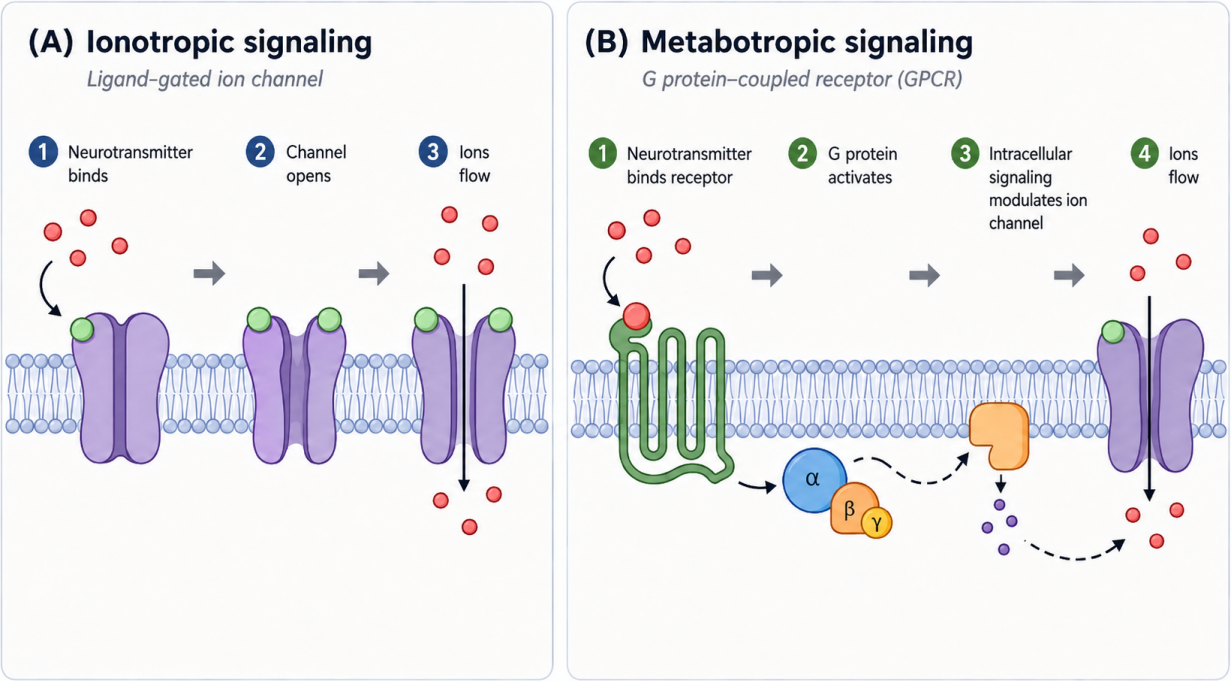

Figure 2.2: Simplified comparison of ionotropic and metabotropic neurotransmitter signaling adapted from [2]. (A) Ionotropic receptors couple neurotransmitter binding more directly to ion-channel activity, whereas (B) metabotropic receptors act through GPCR-mediated intracellular signaling before influencing the cellular responses.

and x_H, then the receptor carries more information about the input. If the responses overlap strongly, then the receptor carries less information.

Ionotropic receptors directly convert neurotransmitter binding into ion-channel activity, while metabotropic receptors act indirectly through GPCR signaling. Because receptor activation is stochastic and state-dependent, receptor behavior can be modeled as transitions among functional states. This biological interpretation motivates the mathematical framework used in the rest of the thesis, where neurotransmitter concentration is treated as the input and receptor state dynamics are treated as the output of a stochastic communication channel. Figure 2.2 highlights the main distinction between ionotropic and metabotropic signaling.

2.1.3 Kinetics and Reaction Rates

Receptor kinetics describe the time-dependent transitions of receptors among functional states, such as unbound, ligand-bound, open, and desensitized states. These transitions

are represented by kinetic schemes in which each state corresponds to a receptor conformation and each arrow corresponds to a rate constant governing the probability of transition per unit time [48]. Because ion-channel receptors behave stochastically, their dynamics are often modeled using continuous-time Markov models, where receptor states and transition rates define the kinetic behavior of the channel [54]. For example, consider a simple ligand-binding reaction:

$$A + R \underset{k_-}{\overset{k_+}{\rightleftharpoons}} AR, \tag{2}$$

where A is a ligand, R is a receptor, and AR is the ligand-bound receptor complex. The forward rate constant k_+ describes ligand association, while the reverse rate constant k_- describes ligand dissociation. Since binding requires the ligand to encounter the receptor, the effective forward binding rate depends on the ligand concentration:

$$k_{\text{bind}} = k_+[A]. \tag{3}$$

Here, $[A]$ denotes the concentration of the ligand. This means that higher ligand concentration generally increases the probability of receptor binding per unit time.

In receptor modeling, kinetic schemes describe the possible states of a receptor and the rates of transition between those states. These states may include resting, ligand-bound, open, and desensitized conformations. Each arrow in a kinetic scheme represents a possible transition, and each transition is assigned a rate constant. Such kinetic models are widely used in neuroscience because many synaptic and ion-channel processes can be represented through state transitions governed by kinetic rates [48].

In this thesis, neurotransmitter concentration acts as the input to the receptor system. The concentration mainly affects ligand-binding transitions, while other kinetic rates describe receptor-specific processes such as unbinding, opening, closing, or desensitization. Therefore, a receptor can be viewed as a stochastic dynamical system whose transition behavior depends on the input concentration.

2.2 Mathematical Background

This section introduces the mathematical tools used to analyze receptor signaling as a stochastic communication process. The first part introduces information-theoretic tools that measure uncertainty and input-output dependence. The second part introduces Markov chains, which are used to model stochastic transitions among receptor states.

2.2.1 Information Theory

Information theory provides a mathematical framework for studying uncertainty, communication, and information transfer. It was originally developed for engineered communication systems, but its concepts are also useful for biological systems because many biological processes involve noisy input-output relationships. In cellular and biochemical signaling, information theory can be used to quantify how much information about an input signal is preserved in a biological response [19].

In this thesis, the input signal is the neurotransmitter concentration, and the output is the receptor response generated by the kinetic model. The goal is to quantify how much information about the input concentration can be inferred from the receptor state dynamics. This is useful because receptor signaling is stochastic: the same concentration may not always produce the same state trajectory, and different concentrations may sometimes produce overlapping receptor responses.

The most basic quantity in information theory is **entropy**. Entropy measures the uncertainty of a random variable. For a discrete random variable X with probability mass function $p(x)$, entropy is defined as

$$H(X) = -\sum_{x} p(x) \log_2 p(x). \tag{4}$$

When the logarithm is base 2, entropy is measured in bits. If one outcome is almost certain, the entropy is low. If several outcomes are possible with similar probabilities, the entropy is higher [16].

For the binary concentration model used in this thesis, the input is written as

$$X \in \{x_L, x_H\}, \tag{5}$$

where x_L is the low neurotransmitter concentration and x_H is the high neurotransmitter concentration. If the probability of the low concentration is p_L, then the probability of the high concentration is $1 - p_L$. The entropy of this binary input is

$$H(X) = -p_L \log_2(p_L) - (1 - p_L) \log_2(1 - p_L). \tag{6}$$

This quantity represents the uncertainty in the input concentration before observing the receptor response.

Conditional entropy measures the remaining uncertainty about one variable after observing another variable. For two random variables X and Y, it is defined as

$$H(X|Y) = -\sum_{x,y} p(x, y) \log_2 p(x|y). \tag{7}$$

In this thesis, X represents the input concentration and Y represents the receptor output. Therefore, $H(X|Y)$ measures how much uncertainty remains about the input concentration after observing the receptor response.

Mutual information measures how much observing one variable reduces uncertainty about another. It is defined as

$$I(X; Y) = H(X) - H(X|Y). \tag{8}$$

Equivalently,

$$I(X; Y) = \sum_{x,y} p(x, y) \log_2 \frac{p(x, y)}{p(x)p(y)}. \tag{9}$$

In the receptor-signaling interpretation, mutual information measures how much the receptor output tells us about the neurotransmitter concentration. If the receptor responses for x_L and x_H are clearly distinguishable, then the mutual information is high. If the receptor behaves similarly under both concentrations, then the mutual information is low.

Channel capacity is the maximum mutual information over all possible input distribu-

tions. For the binary input case, this can be written as

$$C = \max_{p_L} I(X;Y). \tag{10}$$

Here, p_L is varied to find the input distribution that gives the highest information transmission. In this thesis, channel capacity is interpreted as the maximum amount of information that a receptor model can transmit for a given pair of low and high concentrations.

Because receptor dynamics evolve over time, information transmission is not only determined by how much information the receptor response carries about the input concentration, but also by how quickly this information is transmitted. Mutual information measures the information shared between an input and an output over an observation window. However, receptor signaling is a dynamic process, so the same amount of information can have a different interpretation depending on the time scale over which it is transmitted. For this reason, this thesis uses **mutual information rate (MIR)**, which expresses mutual information per unit time.

For an input sequence $X^n = (X_1, \ldots, X_n)$ and an output receptor-state sequence $Y^n = (Y_1, \ldots, Y_n)$, the MIR can be written as

$$\text{MIR} = \lim_{n\to\infty} \frac{1}{n\Delta t} I(X^n; Y^n), \tag{11}$$

where Δt is the simulation time step. This quantity measures the average mutual information per second between the input concentration sequence and the receptor output sequence.

In this work, the input is usually binary, meaning that the receptor is stimulated by either a low concentration, x_L, or a high concentration, x_H. For each input probability p_L, where p_L denotes the probability of applying the low concentration, the model computes an MIR value in bits per second. Therefore, MIR represents how much information per second the receptor-state sequence carries about the input concentration sequence.

For each fixed concentration pair (x_L, x_H), the MIR depends on the input balance p_L. The reported $\text{MIR}_{\max}$ is the largest MIR obtained after optimizing over p_L, and the corresponding p_L^* indicates the input probability that achieves this maximum. In this sense, $\text{MIR}_{\max}$ represents the binary-input channel capacity for that fixed pair of concentrations. Although

a binary input can carry at most one bit per time step, the MIR can be much larger than one bit per second because the simulation uses a very small time step, $\Delta t = 2 \times 10^{-6}$ s. Therefore, the binary-input upper bound is

$$\frac{\log_2(2)}{\Delta t} = \frac{1}{2 \times 10^{-6}} = 500{,}000 \text{ bits/s}, \tag{12}$$

and the MIR values reported in this work remain well below this theoretical limit.

2.2.2 Markov Chains

A Markov chain is a stochastic model used to describe systems that move among a set of states (e.g., a receptor). The defining assumption is the Markov property: the future state depends only on the current state and not on the full history of previous states. This makes Markov chains suitable for modeling receptor kinetics, where a receptor is assumed to occupy one state at a time and transition probabilistically to other states.

Here, receptor kinetic schemes are represented as continuous-time Markov chains. Each receptor state corresponds to a biological or functional state, such as resting, bound, open, or desensitized. Each transition between states is associated with a rate constant. These rate constants determine how likely the receptor is to move from one state to another per unit time. Some of these transitions depend on the input (ligand concentration), which are called sensitive transitions, and the rest are insensitive [10].

A continuous-time Markov chain is described by a generator matrix, denoted by Q. For a receptor with n states, Q is an $n \times n$ matrix. The off-diagonal entry Q_{ij} represents the transition rate from state i to state j:

$$Q_{ij} \geq 0, \qquad i \neq j. \tag{13}$$

The diagonal entries are chosen so that each row sums to zero:

$$Q_{ii} = -\sum_{j \neq i} Q_{ij}. \tag{14}$$

Thus, the generator matrix contains all transition-rate information for the receptor model.

Rate constants

Parameter	Value	Unit
$k_{+2}x$	5×10^8	$M^{-1}s^{-1}$
α_1	3×10^3	s^{-1}
$2k^*_{-2}$	0.66	s^{-1}
α_2	5×10^2	s^{-1}
β_2	1.5×10^4	s^{-1}
$2k_{-2}$	4×10^3	s^{-1}
β_1	15	s^{-1}
$k_{+2}x$	5×10^8	$M^{-1}s^{-1}$
k_{-1}	2×10^3	s^{-1}
$2k_{+1}x$	1×10^8	$M^{-1}s^{-1}$

State transitions

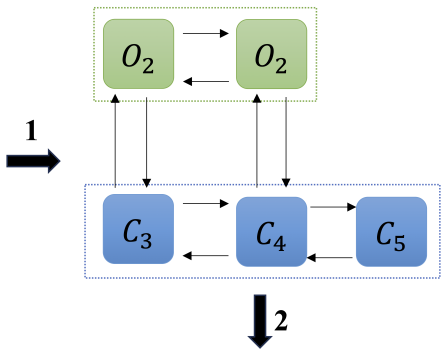

Generator Q matrix

$$Q = \begin{bmatrix} Q_{11} & k_{+2}x & 0 & \alpha_1 & 0 \\ 2k^*_{-2} & Q_{22} & \alpha_2 & 0 & 0 \\ 0 & \beta_2 & Q_{33} & 2k_{-2} & 0 \\ \beta_1 & 0 & k_{+2^x} & Q_{44} & 0 \\ 0 & 0 & 0 & 2k_{+1}x & Q_{55} \end{bmatrix}$$

Figure 2.3: Example conversion of receptor rate constants into state transitions and the corresponding generator matrix Q for a continuous-time Markov chain. Adapted from [10].

This is the standard representation of a continuous-time Markov chain, where the rate matrix defines how the process jumps between states over continuous time [10]. Figure 2.3 shows how the rate constants of a receptor model are translated into state transitions and then organized into the generator matrix Q. This representation shows how the continuous-time Markov chain captures all possible receptor-state transitions and their corresponding rates.

For numerical computation, the continuous-time model can be converted into a discrete-time transition probability matrix over a small time step Δt. This is done using the matrix exponential:

$$P = \exp(Q\Delta t). \tag{15}$$

The entry P_{ij} gives the probability that the receptor moves from state i to state j during one time step. The relationship between the generator matrix and the transition probability

matrix through the matrix exponential is a standard property of continuous-time Markov chains [55]. This input-dependent Markov model connects the biological receptor system to the information-theoretic framework. The neurotransmitter concentration determines the transition rates, the transition rates determine the receptor state dynamics, and the receptor state dynamics form the output process used to compute MIR. A Markov chain is used when the state of the system is directly represented and the next state depends only on the current state. In this thesis, this means that receptor kinetics can be modeled as transitions among receptor states such as resting, bound, open, and desensitized states.

2.2.3 Hidden Markov Models

A hidden Markov model (HMM) is an extension of a Markov chain in which the underlying state sequence is not directly observed. Instead, the system produces observable outputs that depend probabilistically on hidden states. In a standard Markov chain, the model state is treated as *directly available*. In an HMM, the true state must be *inferred* from noisy observations. Rabiner's tutorial is a standard reference for this distinction and presents the main HMM problems, including likelihood evaluation, state decoding, and parameter learning [56].

This distinction is useful for receptor modeling. In the kinetic models used in this thesis, receptor states such as closed, open, and desensitized states are explicitly defined by the kinetic scheme. Therefore, the receptor can be modeled directly as a Markov chain. However, in experimental settings, the true receptor state is often not directly observed. For example, single-channel recordings measure noisy ionic current traces, while the underlying open and closed states must be inferred. In such cases, HMMs provide a natural framework for estimating hidden receptor or ion-channel states from observed data [57].

3 Information-Theoretic Analysis of Dopamine and Serotonin Signaling at the Human 5-HT$_{3A}$ Receptor

Serotonin type 3 (5-HT$_3$) receptors are expressed throughout the central nervous system in areas governing the vomiting reflex, pain processing, the reward system, cognition, and anxiety regulation. Peripherally, they are found on various neurons and immune cells. Their involvement spans a range of conditions including emesis, pain disorders, drug addiction, and both psychiatric and gastrointestinal disorders [6, 58].

Neurotransmitter receptors fall into two main families. Ionotropic receptors are fast-acting, where neurotransmitter binding directly opens an ion channel within the same protein. Metabotropic receptors, in contrast, act indirectly through G-proteins and intracellular signaling to influence ion channels more slowly [2]. Unlike other serotonin (5-HT) receptors (5-HT$_1$ to 5-HT$_7$), which rely on G-protein signaling, the 5-HT$_3$ receptor functions as an ionotropic ligand-gated ion channel (LGIC). It belongs to the Cys-loop LGIC family alongside glycine, GABA$_A$, and nicotinic acetylcholine (nACh) receptors (a family characterized by a conserved architecture of five pseudo-symmetrically arranged subunits encircling a central ion-conducting pore) [1, 59].

High concentrations of 5-HT can activate nearly all 5-HT$_3$ receptors. Upon agonist (a substance that binds to and activates a receptor) removal, currents decline through deactivation, while prolonged exposure causes reversible desensitization, rendering receptors temporarily unresponsive. Notably, dopamine (DA) can also activate 5-HT$_3$ receptors [6].

This work analyzes 5-HT and DA neurotransmitter signaling through an information-theoretic lens, using the 5-HT$_{3A}$ receptor as the model system, building on Shannon's foundational communication framework [60]. The "A" in 5-HT$_{3A}$ refers to a specific subunit of the 5-HT$_3$ receptor and is the primary subunit capable of forming a functional receptor on its own [1]. Neurons communicate via neurotransmitters that bind to receptors (either fast-acting ionotropic receptors or slower metabotropic GPCRs [1, 2], and these signaling processes can be modeled as communication channels. DA acts through five GPCR subtypes (D$_1$ to D$_5$) [61], while 5-HT has at least 14 subtypes across seven families, nearly all GPCRs except the ion channel 5-HT$_3$ [1]. This study focuses on the 5-HT$_{3A}$ receptor using kinetic

parameters from [6].

Information-theoretic methods are well-suited for this analysis because they are model-independent, handle linear and nonlinear interactions, and allow cross-system comparisons in bits [17, 19, 23, 24]. Prior work has applied these tools to biochemical noise [17, 24], synaptic capacity [29, 41], molecular communication [62], and neurological disorders [63, 64], but to the best of our knowledge, no prior work has compared DA and 5-HT using MIR within a unified receptor-kinetic framework at the human 5-HT_{3A} receptor. Extending prior channel-capacity analysis of receptors like Channelrhodopsin-2, nicotonic Acetylcholine, and Calmodulin [10], this work computes MIRs for neurotransmitter receptor systems, examines how concentration and kinetic transitions affect information throughput, and proposes a general framework for applying information theory to neurotransmitter signaling.

Information theory can be used to formulate testable hypotheses about biological systems, which are often hypothesized to operate near their theoretical limits [26, 65]. This motivates the use of MIR as a measure of signaling efficiency in this work.

The remainder of this chapter is organized as follows. Section 3.1 presents the system model for serotonin and dopamine signaling at the human 5-HT_{3A} receptor. This section describes the biochemical signaling mechanism, introduces the receptor-state kinetic model derived from prior experimental work, and formulates the corresponding master equation for the stochastic receptor-state dynamics. Section 3.2 describes the methodology used to construct the transition-rate matrix and compute the MIR from the receptor kinetics. Section 3.3 visualizes the MIR analysis, including the effects of input probability, concentration regimes, and concentration ratio on information transmission. Section 3.4 discusses the main findings and their implications for receptor-level information processing. Finally, the chapter concludes by summarizing the main findings and outlining directions for future research.

3.1 System model

Receptor dynamics describe how receptor proteins transition between different conformational states over time in response to ligand binding. These processes are commonly represented using kinetic models, where the receptor is modeled as a system that moves between states such as resting, open, and desensitized [6]. Each transition occurs with a specific

rate determined by biochemical processes such as ligand binding, channel opening, closing, and desensitization. Such models are often formulated as stochastic continuous-time Markov processes, which provide a mathematical framework for describing the temporal evolution of receptor states and predicting macroscopic receptor responses [10].

3.1.1 Physical model

DA and 5-HT are two important biogenic amine neurotransmitters, a group of small-molecule neurotransmitters derived from amino acids that regulate many neural processes including reward, mood, and cognition [2]. DA receptors consist of five known subtypes (D_1–D_5), all of which belong to the G protein–coupled receptor (GPCR) family and produce slower intracellular signaling responses through second-messenger pathways. In contrast, 5-HT receptors are more diverse and include seven receptor families (5-HT_1–5-HT_7). Most 5-HT receptors are also GPCRs; however, the 5-HT_3 receptor is unique because it is an ionotropic receptor, meaning it functions as a ligand-gated ion channel. When activated, ion channels allow ions to flow directly across the membrane, producing fast postsynaptic responses on the order of milliseconds [1].

The ionotropic nature of the 5-HT_3 receptor makes it particularly suitable for information-theoretic analysis [66], since the receptor can be naturally modeled as a stochastic state-transition system whose states correspond to different channel conformations (such as resting, open, and desensitized states) [67]. Experimental studies have shown that both 5-HT and DA can interact with the 5-HT_{3A} receptor, but they produce different kinetic behaviors. In particular, 5-HT acts as a strong agonist that rapidly opens the ion channel and produces sustained currents, whereas DA interacts more weakly and generates slower activation with faster dissociation dynamics [6]. These differences in receptor kinetics play an important role in determining how effectively the receptor can transmit information about neurotransmitter concentration, which motivates the information-theoretic analysis performed in this work.

The receptor-state transitions are illustrated in Figure 3.1, where each node represents a receptor conformation and edges correspond to kinetic transitions between states. The scheme is adapted from Solt et al. [6] with minor modifications: low-probability transitions (shown in grey in the original model) are omitted, and only the major states and transitions

(shown in black in the original model) necessary to capture the actions of 5-HT and DA on the human 5-HT$_{3A}$ receptor are included. The receptor states in Figure 3.1 can be understood in terms of three functional configurations: resting (R), open (O), and desensitized (D). Within each configuration, states of the form A_kX ($k = 0, 1, 2, 3$ and $X \in \{R, O, D\}$) indicate the number of bound ligand molecules. The top row (R, AR, A_2R, A_3R) represents closed resting states with increasing ligand occupancy. The middle row (O, AO, A_2O, A_3O) corresponds to open, conducting states through which ions can pass, while the bottom row (D, AD, A_2D, A_3D) captures desensitized states, where the receptor remains ligand-bound but no longer conducts.

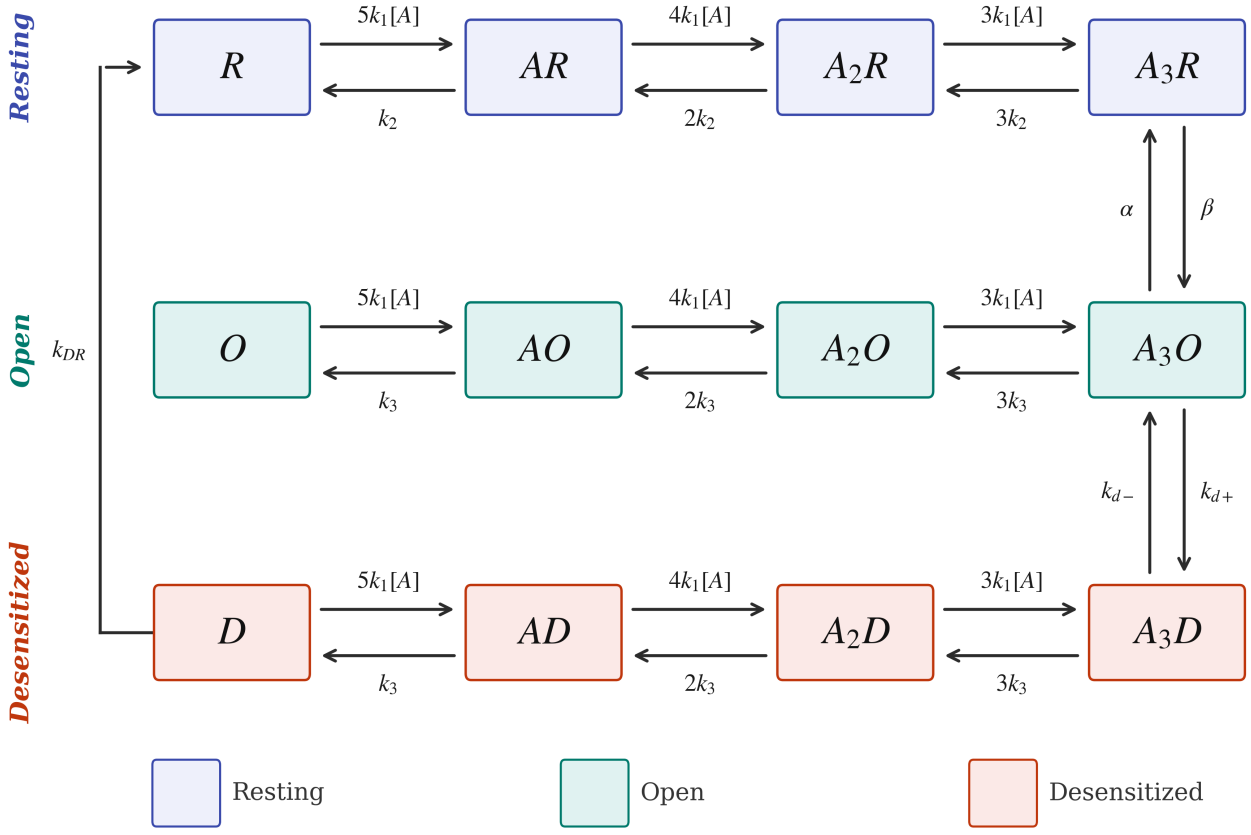

Figure 3.1: Kinetic scheme for human 5-HT$_{3A}$ receptor function, adapted from [6]. In each configuration, A is the ligand and A_kX ($k = 0, 1, 2, 3$ and $X \in \{R, O, D\}$) denotes a state with k ligand molecules bound.

The corresponding kinetic rate constants for both neurotransmitters are listed in Table 3.1. Among these, only the ligand-binding transitions are *input-sensitive*, since their rates scale with the concentration through terms of the form $k_1[A]$. All other transitions are *input-*

insensitive, as they describe input-independent receptor dynamics such as unbinding, gating, and desensitization, and therefore do not depend on the input (insensitive).

Parameter	**5-HT**	**DA**
k_1	1×10^7 $M^{-1}s^{-1}$	1×10^7 $M^{-1}s^{-1}$
k_2	200 s^{-1}	1700 s^{-1}
k_3	0.207 s^{-1}	14 s^{-1}
β	400 s^{-1}	0.6 s^{-1}
α	1 s^{-1}	1.2 s^{-1}
k_{d+}	1.15 s^{-1}	1.15 s^{-1}
k_{d-}	< 0.01 s^{-1}	< 0.01 s^{-1}
k_{DR}	0.7 s^{-1}	0.7 s^{-1}

Table 3.1: Kinetic rate constants of 5-HT and DA at the human 5-HT_{3A} receptor derived from [6]. The parameter L_0 defines the equilibrium ratio between unliganded resting and open states $[R]/[O]$, but [6] do not provide explicit kinetic rates for the corresponding transition $R \leftrightarrow O$, instead treating L_0 as a thermodynamic constraint. We tested several plausible implementations of this transition and observed no significant change in the MIR. Therefore, we chose to omit the unliganded gating transition and ignore L_0 in the final model.

3.1.2 Mathematical model

The biological and mathematical foundations of receptor signaling were introduced in Section 2. Therefore, this section only summarizes how those concepts are applied to the 5-HT_{3A} receptor model analyzed in this chapter.

The receptor is modeled as a finite-state continuous-time Markov chain, where each state represents a receptor conformation such as resting, open, or desensitized. As described in Section 2.1, the input signal is the ligand concentration, denoted by $x(t)$. For an N-state receptor model, the state probability vector is

$$\mathbf{p}(t) = \big[p_1(t), p_2(t), \ldots, p_N(t)\big], \tag{16}$$

and its time evolution is governed by

$$\frac{d\mathbf{p}(t)}{dt} = \mathbf{p}(t)Q(x(t)). \tag{17}$$

Here, $Q(x(t))$ is the input-dependent generator matrix. The off-diagonal entry $q_{ij}(x(t))$ gives

the transition rate from state i to state j, and the diagonal entries are chosen so that each row sums to zero:

$$q_{ii}(x(t)) = -\sum_{j \neq i} q_{ij}(x(t)). \tag{18}$$

As discussed in Section 2.2, some transitions are input-sensitive, meaning that their rates depend on ligand concentration, while other transitions are input-insensitive and remain fixed. In ligand-gated receptor models, binding transitions are typically concentration-dependent, whereas opening, closing, unbinding, and desensitization transitions are governed by intrinsic kinetic parameters.

For numerical computation, the continuous-time model is converted into a discrete-time transition probability matrix using the matrix exponential:

$$P(x) = e^{Q(x)\Delta t}, \tag{19}$$

where $\Delta t = 0.002$ ms in the simulations. As introduced in Section 2.2, the entry $P_{ij}(x)$ gives the probability of transitioning from state i to state j during one time step under input concentration x. Small numerical errors from the matrix exponential are corrected by clipping negative values and renormalizing each row so that $P(x)$ remains a valid stochastic matrix.

To compute the MIR, the input alphabet is defined as

$$\mathcal{X} = x_1, \ldots, x_m, \tag{20}$$

with input probabilities $p(x_i)$. Under an IID input distribution, the averaged receptor transition matrix is

$$\bar{P} = \sum_{x_i \in \mathcal{X}} p(x_i) P(x_i), \tag{21}$$

and the stationary distribution π is obtained from

$$\pi \bar{P} = \pi, \qquad \sum_{y} \pi_y = 1. \tag{22}$$

The information-theoretic definitions of mutual information, channel capacity, and MIR

were given in Section 2.2. In this chapter, these quantities are computed for the receptor-state sequence generated by the Markov model. A useful simplification is that, under IID inputs, only the input-sensitive transitions contribute to the MIR; input-insensitive transitions do not contribute because their probabilities are independent of the input.

Let S denote the set of sensitive transitions in the receptor-state graph, and define $\phi(p) = p \log_2 p$ for $p \neq 0$ and $\phi(0) = 0$. Following Theorem 1 of Eckford and Thomas [10], the mutual information per time step is computed as

$$I_{\Delta t}(X;Y) = \sum_{(y_{i-1},y_i)\in S} \pi_{y_{i-1}} \left[\sum_{x_i \in \mathcal{X}} p(x_i)\phi\left(p(y_i \mid x_i, y_{i-1})\right) \quad -\phi\left(\sum_{x_i \in \mathcal{X}} p(x_i) p(y_i \mid x_i, y_{i-1}) \right) \right]. \tag{23}$$

Here, $p(y_i \mid x_i, y_{i-1})$ is obtained from the transition matrix $P(x_i)$. The MIR in bits per second is then obtained by normalizing this value by the time step Δt.

3.2 Methodology

The 5-HT_{3A} receptor state space and kinetic parameters are based on the experimental patch-clamp study of Solt et al. [6], which characterized the differential effects of 5-HT and DA on the receptor using a multi-state kinetic scheme. The model contains $N = 12$ receptor states, including unliganded resting states, singly- through triply-liganded closed states, an open conducting state, desensitized states, and a deep-desensitized state. For simplicity, the grey transitions identified in Solt et al. are excluded from the implementation.

For each neurotransmitter and ligand concentration x, the corresponding generator matrix $Q(x) \in \mathbb{R}^{12\times 12}$ is constructed from the rate constants listed in Table 3.1. Ligand-sensitive transitions depend on concentration, while input-insensitive transitions remain fixed. In this model, ligand-binding transitions scale linearly with x; for example, the transition from the unbound state to the first bound state is proportional to $5k_1x$. Other kinetic processes, including gating and desensitization, are treated as concentration-independent.

The input is modeled using a binary concentration alphabet, with a low concentration x_L and a high concentration x_H. For each concentration pair, the input probability p_L is varied, with $p_H = 1 - p_L$. To examine how the input concentration range affects information trans-

mission, four biologically motivated scenarios are evaluated, each defined by a pair (x_L, x_H) for each neurotransmitter. Here, EC_{50} means the half-maximal effective concentration.

1. *Sub-EC_{50}* — $x_H = 1\,\mu$M for 5-HT and $x_H = 50\,\mu$M for DA, corresponding to 0.4× and 0.25× their respective EC_{50} values [6].

2. *Near-EC_{50}* — $x_H = 3\,\mu$M for 5-HT and $x_H = 200\,\mu$M for DA, corresponding to 1.2× and 1.0× their respective EC_{50} values [6].

3. *Solt experimental* — concentration bounds taken directly from [6]: 5-HT at [0.3 μM, 1000 μM], DA at [30 μM, 2000 μM].

4. *In vivo multi-region* — concentration bounds are derived from experimentally reported extracellular measurements in rodent models across multiple brain regions, capturing both baseline and elevated activity levels. For 5-HT, the range $[0.18 \times 10^{-3}\mu\text{M}, 68 \times 10^{-3}, \mu\text{M}]$ is adopted from [13]. For DA, the range [0.02 μM, 0.2 μM] is used, where the lower bound (x_L) is based on microdialysis measurements reported in [11], and the upper bound (x_H) reflects elevated transient concentrations observed using fast electrochemical techniques [12]. This regime is included to evaluate how biologically realistic variability in neurotransmitter concentrations impacts information transmission.

For each scenario, the MIR is evaluated over 1000 uniformly spaced values of $p_L \in (0, 1)$, and the peak MIR I^*_{rate} together with the corresponding optimal prior p^*_L are recorded for both 5-HT and DA.

3.3 MIR Analysis

In this section, we investigate how the MIR changes under different input concentration settings. Specifically, we investigate two main questions:

1. In Section 3.3.1, we investigate how the input probability p_L, which represents the probability of the low concentration x_L, affects the MIR for a fixed concentration pair (x_L, x_H).

2. In Section 3.3.2, we analyze how the concentration ratio x_H/x_L, which represents the contrast between the high and low input concentrations, affects the MIR. In particular, we examine whether increasing this ratio continuously improves information transmission, or whether the MIR reaches an optimal range before decreasing, saturating, or converging to a specific value for each of our receptors.

3.3.1 Effect of Input Probability p_L on MIR

Figures 3.2a and 3.2b show the MIR (bits/s) as a function of p_L for 5-HT and DA, respectively, across all four concentration cases. In both figures, the MIR follows the same qualitative shape: it rises from zero, peaks at some intermediate p_L^*, and then falls sharply back toward zero as $p_L \to 1$. This pattern is not surprising. When the input collapses to a point at either extreme, the channel carries no uncertainty and therefore no information [60].

Across all cases, the optimal p_L^* ranges from ≈ 0.6–0.9, indicating that the receptor extracts the most information when high-concentration events are relatively rare. This is consistent with how DA and 5-HT actually behave in the brain. Both systems operate in a phasic regime, punctuated by brief concentration transients above a low tonic baseline [12, 68].

These trends are summarized in Table 3.2, which reports the peak MIRs and corresponding optimal input distributions. The table highlights two consistent patterns across all regimes: (i) the optimal input distribution is skewed toward low concentrations ($p_L^* > 0.5$), and (ii) the achievable MIR varies significantly with both the concentration range and neurotransmitter kinetics.

For both 5-HT and DA, the Solt experimental case produces the largest MIR, followed by the near-EC_{50} and sub-EC_{50} cases. The peak generally occurs when p_L is close to one, which means that the low-concentration state is dominant and high-concentration events are highly rare. This suggests that, in these regimes, the receptor output carries the most information when occasional high-input events are embedded within a mostly low-input background.

For 5-HT, the Solt experimental case reaches the highest MIR, with a sharp peak near $p_L \approx 1$. The near-EC_{50} case produces a smaller but still clear peak, while the sub-EC_{50} case remains much lower across the full range of p_L. This indicates that larger separation between the low and high concentration levels leads to higher MIR.

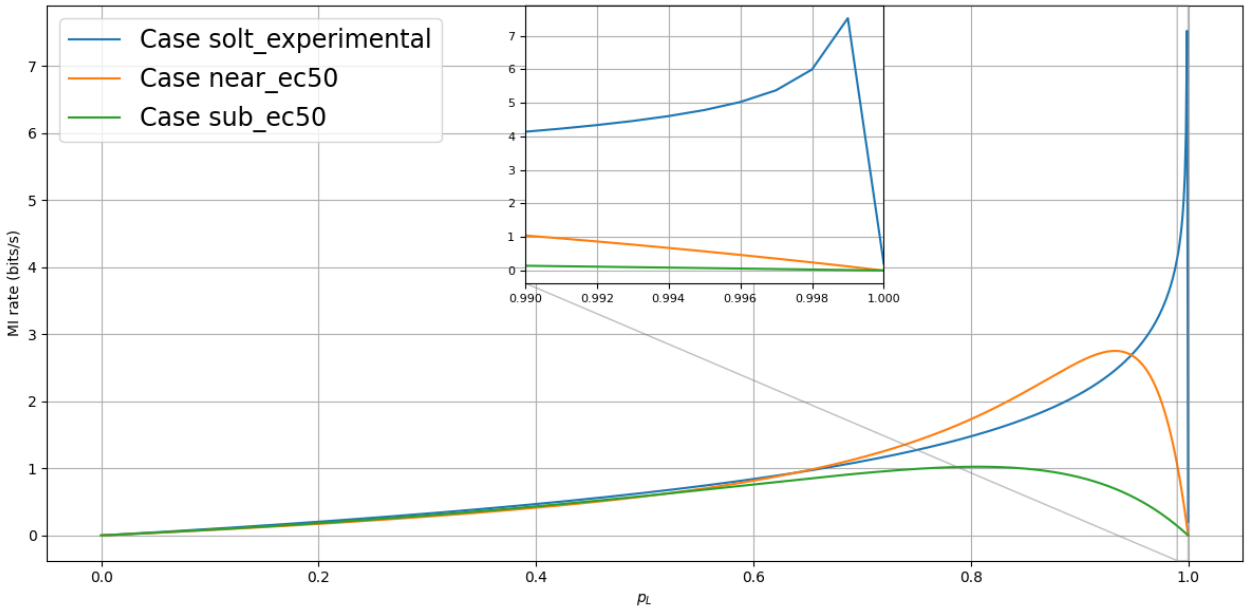

(a) 5-HT

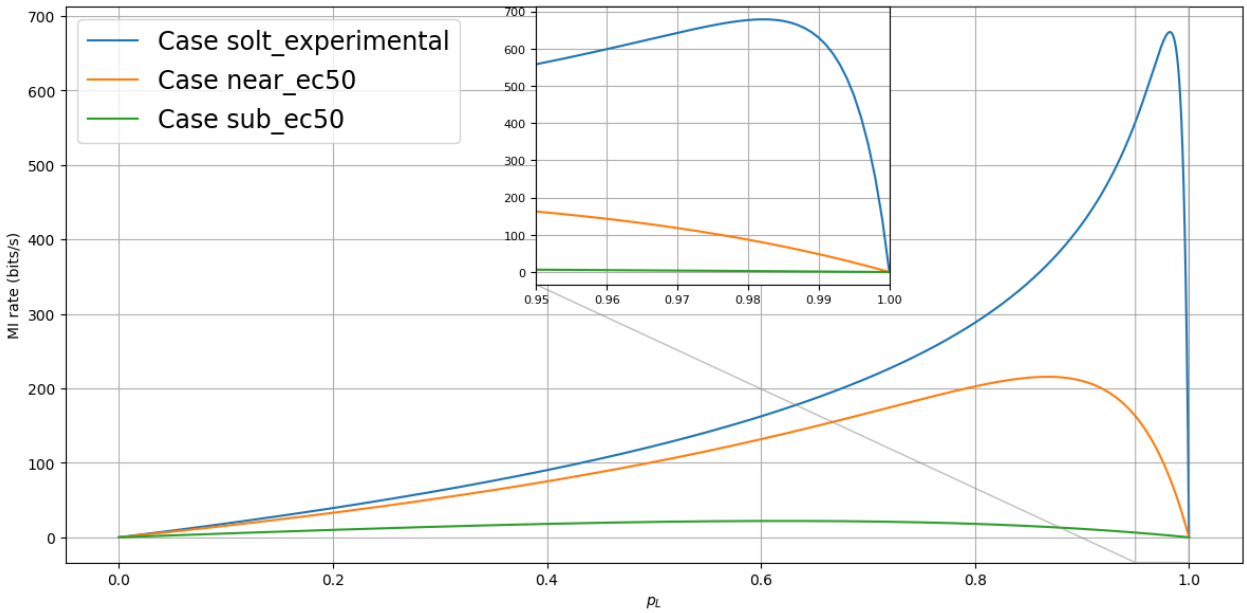

(b) DA

Figure 3.2: MIR for (a) 5-HT and (b) DA at the human 5-HT_{3A} receptor for three concentration regimes based on [6]: sub-EC_{50} (concentrations below the half-maximal effective concentration (EC_{50})), near-EC_{50} (concentrations close to EC_{50}), and Solt experimental (exact concentrations reported in the study). The time step is dt = 0.002 ms. In all cases, the MIR is zero at $p_L = 0$ and $p_L = 1$, where the input is deterministic and the channel carries no information. For both plots, an inset subplot highlights the behavior near $p_L = 1$.

The same overall pattern appears for DA, but with a much larger scale. Under the kinetics provided in Table 3.1, DA reaches substantially higher MIRs than 5-HT in the corresponding experimental and EC_{50}-based regimes. This gap is not explained only by the input concentration ranges; it also reflects the different kinetic parameters of DA at the same 5-HT_{3A} receptor architecture. This means that DA produces more distinguishable receptor responses at low and high inputs, which increases the MIR.

For the in vivo multi-region case, the behavior is different from the previous ones. Both neurotransmitters show smooth, moderate MIR curves with peaks around intermediate values of p_L, rather than sharp peaks near $p_L = 1$. DA still achieves a higher MIR than 5-HT, but the difference is much smaller than in the previous ones. This suggests that, under more physiologically realistic extracellular concentration ranges, the information gap between DA and 5-HT is reduced.

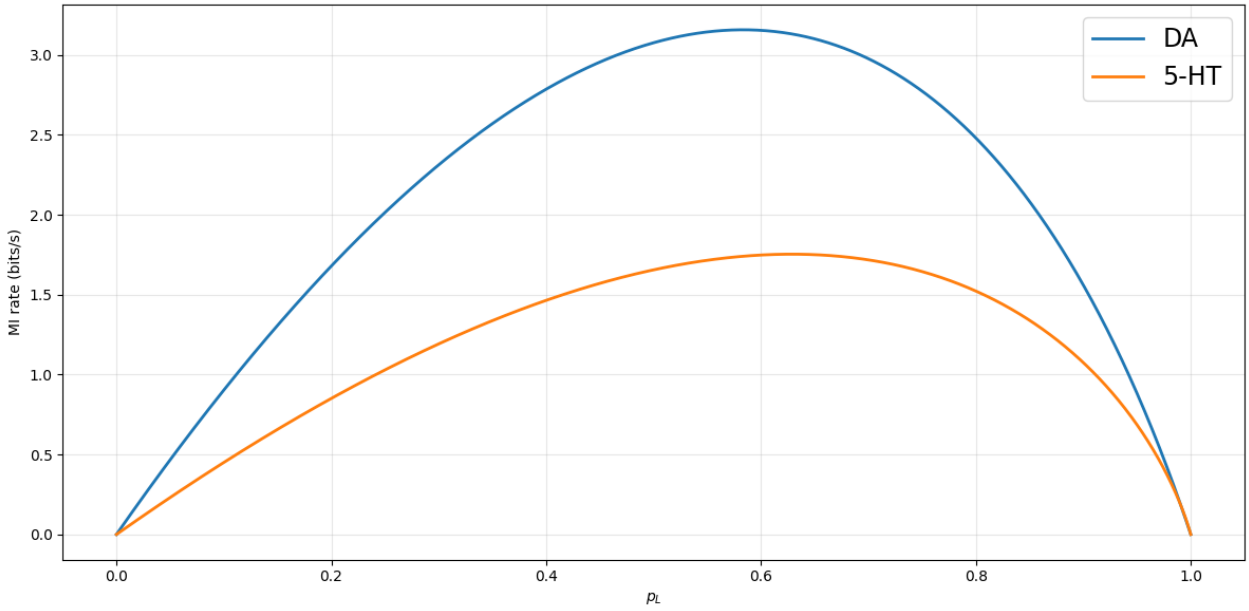

Figure 3.3: MIR for 5-HT and DA at the human 5-HT_{3A} receptor in the in vivo multi-region regime. The blue curve corresponds to DA and the orange curve to 5-HT. Concentration bounds are based on experimentally reported extracellular measurements across brain regions, capturing baseline and elevated activity levels: DA in [0.02, 0.2] μM [11, 12], and 5-HT in $[0.18 \times 10^{-3}, 68 \times 10^{-3}]$ μM [13].

Table 3.2: Peak MIR across concentration regimes. Concentrations are reported in μM and MIRs in bits/s.

Regime	**Ligand**	x_L	x_H	p_L^*	$MIR_{\max}$
Sub-EC50	5-HT	0.3	1	0.807	1.025
	DA	30	50	0.621	22.000
Near EC50	5-HT	0.3	3	0.933	2.752
	DA	30	200	0.868	215.500
Solt et al. experimental	5-HT	0.3	1000	0.999	7.524
	DA	30	2000	0.982	678.400
In vivo multi-region	5-HT	0.18×10^{-3}	68×10^{-3}	0.629	1.753
	DA	0.02	0.2	0.584	3.157

3.3.2 Effect of the Concentration Ratio x_H/x_L on MIR

To investigate how the discriminability of two concentrations scales with their separation, we fixed the low concentration x_L for each ligand and varied the high concentration as $x_H = c \cdot x_L$, sweeping the ratio c logarithmically in the range of $(10^0$–$10^7)$ across 80 points. For each value of c, we computed the peak MIR rate over all prior probabilities $p_L \in (0, 1)$, as well as the optimal prior p_L^* that achieves it.

Peak MIR: The two ligands exhibit qualitatively distinct responses to increasing c. For 5-HT (with $x_L = 0.3$ μM), the peak MIR rises monotonically until $c \approx 840$, at which point $x_H \approx 252$ μM, and reaches a maximum of 10.70 bits/s. Beyond this optimum, the MIR drops sharply by 42% to a trough of 6.20 bits/s at $c \approx 1.5 \times 10^4$, before partially recovering to a plateau of ≈ 7.01 bits/s at large c. This plateau represents only 65.5% of the peak, indicating that the 5-HT receptor does not fully recover its discriminative capacity once the concentrations exceed its optimal operating range. This result is shown in Figure 3.4.

For DA (with $x_L = 30$ μM), the behavior is remarkably different. The peak MIR rises steeply, reaching a maximum of 878 bits/s at $c \approx 455$ ($x_H \approx 13,700$ μM), and then decreases only slightly to a stable plateau of ≈ 828 bits/s, retaining 94.3% of its peak value. Compared with 5-HT, the DA model maintains a much higher MIR and remains close to its maximum value across a broad range of large concentration ratios, suggesting that its transition dynamics remain informative over a wider concentration-contrast range. The result for DA is

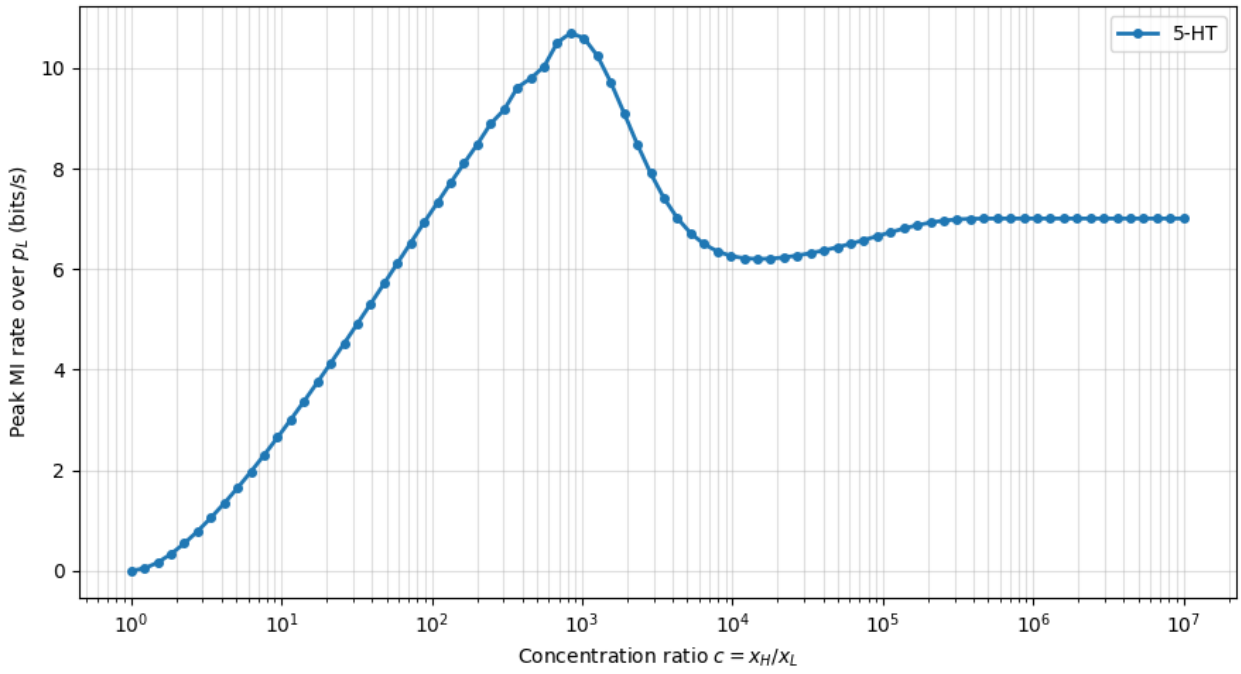

Figure 3.4: Peak MIR versus concentration ratio $c = x_H/x_L$ for the 5-HT_{3A} receptor model with fixed $x_L = 0.3$ μM. The MIR increases with c up to an intermediate optimum of 10.70 bits/s at $c \approx 840$ ($x_H \approx 252$ μM), then decreases and eventually converges to approximately 7.01 bits/s at large ratios. This non-monotonic trend shows that increasing the concentration contrast improves information transmission only up to an optimal range; beyond that, additional increases in x_H produce less distinguishable receptor dynamics and do not further improve MIR.

shown in Figure 3.5.

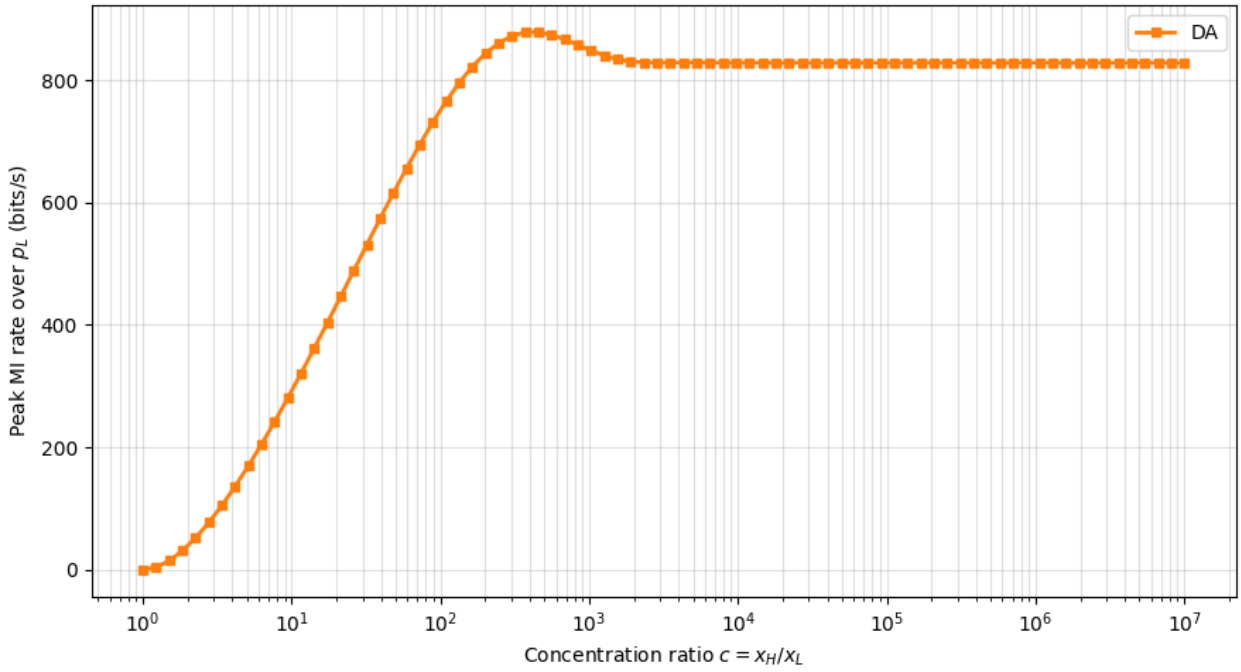

Figure 3.5: Peak MIR versus concentration ratio $c = x_H/x_L$ for DA at the 5-HT$_{3A}$ receptor model with fixed $x_L = 30$ μM. The MIR rises steeply and saturates at ≈ 828 bits/s, retaining 94.3% of its peak value of 878 bits/s reached at $c \approx 455$ ($x_H \approx 13,700$ μM).

Optimal input probability p_L^*: In addition to the peak MIR, we also examined the optimal input probability p_L^*, which represents the probability of the low concentration x_L that maximizes the MIR for each ratio $c = x_H/x_L$. As shown in Figure 3.6, both ligands exhibit a similar trend. When the concentration ratio is small, p_L^* is close to 0.5, meaning that the MIR is maximized when the low and high concentrations are presented with nearly equal probability. This is expected because when x_L and x_H are close, neither input is strongly dominant in terms of information contribution. As the ratio increases, p_L^* rapidly approaches one for both 5-HT and DA. This indicates that, at large concentration contrasts, the MIR is maximized when the low concentration occurs most of the time and the high concentration occurs more rarely. In this regime, the high concentration acts as a rare but highly informative input because it produces receptor transition dynamics that are more distinct from the baseline low-concentration response (Figure 3.6). A summary of all of these results is presented in Table 3.3.

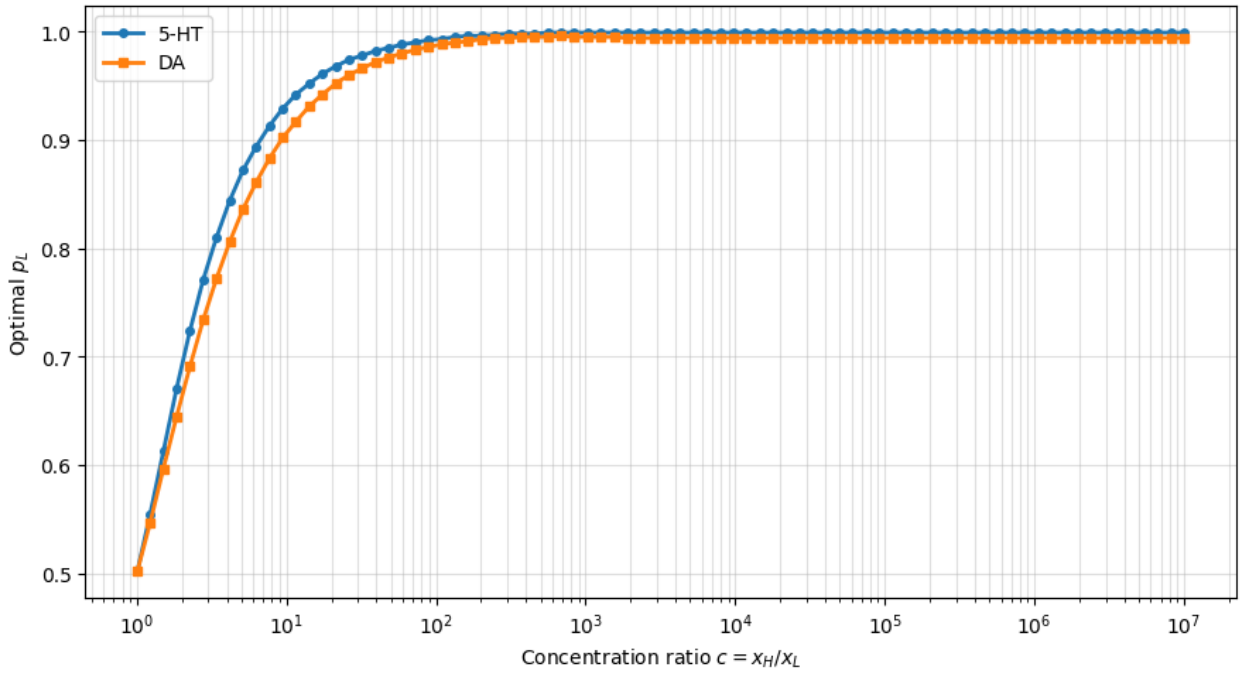

Figure 3.6: Optimal input probability p_L^* as a function of the concentration ratio $c = x_H/x_L$ for 5-HT and DA at the 5-HT_{3A} receptor model. For each value of c, p_L^* is the probability of the low concentration that maximizes the MIR. At small ratios, p_L^* is close to 0.5, indicating a nearly balanced optimal input distribution. As the ratio increases, p_L^* approaches one for both ligands, showing that the MIR is maximized when the low concentration is frequent and the high concentration is rare.

Table 3.3: Summary of controlled concentration ratio sweep for 5-HT and DA.

Metric	**5-HT**	**DA**
Fixed x_L	0.3 μM	30 μM
Peak MIR (bits/s)	10.70	878
c at peak MIR	≈ 840	≈ 455
x_H at peak MIR	≈ 252 μM	$\approx 13,700$ μM
High-c plateau (bits/s)	7.01	828
Plateau as % of peak	65.5%	94.3%
p_L^* at $c = 10^7$	0.999	0.994

These results suggest that neurotransmitter signaling is not simply optimized by making the high concentration as large as possible. Instead, the receptor transmits the most information when the two input concentrations produce sufficiently different, but not fully saturated, receptor dynamics. This is consistent with the general idea that biological systems can be studied as information-processing systems, where information flow depends on how reliably an output state reflects an input signal [19, 23]. Our MIR analysis provides a quantitative way to ask how well receptor state transitions encode changes in neurotransmitter concentration. The observation that the optimal p_L^* approaches one at large x_H/x_L suggests that the model is most informative when the receptor operates near a frequent low-concentration baseline and responds to rare high-concentration events. This interpretation is consistent with the general biological distinction between tonic and phasic signaling, particularly in dopamine systems, where tonic dopamine is often associated with a slower baseline level and phasic dopamine with brief transient elevations [69]. However, in this thesis, the analogy is used only as an interpretation of the model output, not as a direct claim that the simulated input probabilities exactly reproduce physiological dopamine release patterns. Finally, the decrease or saturation of MIR at very large concentration ratios is biologically plausible in light of receptor desensitization. Previous studies describe desensitization in ligand-gated ion channels as a reduction in ionic flux during prolonged agonist exposure, and show that neurotransmitter-gated ion channels can exhibit reduced peak-current responses during repeated high-frequency stimulation [70, 71]. Therefore, while our MIR results do not directly model experimental desensitization protocols, the observed plateau or decline at large x_H/x_L is consistent with the broader idea that receptor responsiveness does not necessarily increase indefinitely with stronger or repeated stimulation.

3.4 Discussion

The large gap in the peak of MIR between DA and 5-HT at the 5-HT_{3A} receptor reflects a fundamental principle: information transmission capacity is governed not by structural identity or binding affinity, but by the kinetic asymmetry between ligands. DA's markedly faster unbinding rate ($k_2 = 1700$ s^{-1} vs. 200 s^{-1} for 5-HT) and accelerated desensitization transition ($k_3 = 14$ s^{-1} vs. 0.207 s^{-1}), combined with a substantially lower channel-opening

rate ($\beta = 0.6$ s^{-1} vs. 400 s^{-1}), produce output-state distributions that differ more sharply between low and high input concentrations. As established in the information-theoretic signaling literature, a larger separation between conditional output distributions at distinct input levels directly increases mutual information [60].

Implications for Pharmacology and Drug Design: A direct translational application of this framework is pharmacological profiling. Any drug acting on the 5-HT$_{3A}$ receptor will alter some subset of the kinetic rate constants in Table 3.1, shifting the MIR in a predictable direction. Compounds that reduce the contrast between conditional output distributions suppress MIR; those that sharpen it enhance signaling fidelity. This provides a scalar, model-independent metric that complements traditional efficacy measures, and could identify compounds that are highly efficacious yet informationally redundant, or modest agonists that nonetheless preserve signaling capacity. Information-theoretic analyses of GPCR signaling pathways have demonstrated that channel capacity is quantifiably reduced in pathological states, motivating its use as a functional biomarker alongside conventional molecular readouts [24]. Analogous frameworks applied to the 5-HT$_{3A}$ receptor could be particularly relevant in disorders such as schizophrenia, treatment-resistant depression, and irritable bowel syndrome, where dopaminergic and serotonergic systems are jointly implicated and therapeutically targeted [58].

Hidden Markov Models (HMMs) and GPCR Systems: A natural extension of this work is to apply the same information-theoretic framework to GPCR-mediated neurotransmitter signaling. Unlike the 5-HT$_{3A}$ receptor, GPCRs do not directly open an ion channel; instead, ligand binding drives conformational changes that regulate downstream G-protein coupling. Hidden Markov models provide a suitable framework for this setting because GPCR signaling can be represented as transitions among latent receptor conformations and signaling states. Prior studies have already shown that HMM-based models can predict GPCR G-protein coupling specificity from receptor sequence[72, 73]. This suggests that future work could connect sequence-based coupling prediction with kinetic state-transition models, allowing information rate to be compared across ionotropic and metabotropic neurotransmitter receptors (GPCRs).

Machine Learning and Data-Driven Models: A second direction is to integrate machine learning with the proposed kinetic-information framework. Recent work has shown that recurrent neural networks can forecast GPCR molecular dynamics trajectories and identify receptor regions with relatively stable or informative motion patterns [74]. This is especially relevant for GPCRs, where signaling depends on conformational dynamics rather than direct channel opening. Public GPCR resources and databases such as GPCRdb and GPCRmd further make it possible to combine receptor sequence, structure, ligand, and molecular-dynamics data at larger scale [75, 76]. Future models could therefore use machine learning to estimate kinetic parameters, classify ligand-specific signaling profiles, or predict how changes in receptor dynamics alter MIR. In this way, the proposed approach could move from a receptor-specific simulation study toward a broader data-driven framework for comparing neurotransmitter signaling more efficiently across receptors.

Other Biologically Important Neurotransmitters: Finally, the framework can be extended beyond DA and 5-HT by applying the same analysis to other neurotransmitter systems. This enables systematic comparison across receptor classes, particularly between ionotropic receptors and cascade-based GPCR systems.

4 Information-Theoretic Analysis of Fast Neurotransmitter Receptor Models

Building on the previous analysis of dopamine and serotonin at the human 5-HT3A receptor, this chapter applies the same information-theoretic framework to three major neurotransmitter systems: glutamatergic, GABAergic, and glycinergic signaling. These systems are especially suitable for this type of analysis because they are ionotropic receptors, whose activity can be represented through discrete kinetic states such as closed, open, and desensitized states. In contrast to many metabotropic or GPCR-based pathways, ionotropic receptors provide a more direct connection between ligand binding, receptor state transitions, and signal transmission.

4.1 Motivation and Chapter Overview

The goal of this chapter is to examine whether different receptor systems show different capacities for transmitting information about changes in ligand concentration. By analyzing all three systems using the same Markov-based and MIR framework, this chapter provides a consistent basis for comparing receptor-level communication across major excitatory and inhibitory neurotransmitter pathways.

4.2 Selection of Receptor Models

This chapter focuses on three major neurotransmitter systems: glutamate, GABA, and glycine. These systems were selected because they are commonly associated with fast ionotropic receptors whose behavior can be described using discrete kinetic states, such as closed, open, bound, and desensitized states [5, 77]. This makes them suitable for continuous-time Markov modeling and MIR analysis [10].

The three neurotransmitters also provide a useful functional comparison. Glutamate is generally considered the main excitatory neurotransmitter in the central nervous system, meaning that it increases the likelihood that a neuron will become active and transmit a signal [3]. In contrast, GABA and glycine are mainly inhibitory neurotransmitters, meaning

that they reduce the likelihood of neuronal activation [78, 79]. In this thesis, these terms are used only to provide biological context; the main focus remains on the computational behavior of the receptor models.

From a modeling point of view, each selected receptor is treated as a state-based communication system. Ligand concentration affects specific transition rates, and these changes alter the probability distribution over receptor states. By converting each receptor model into a transition-rate matrix, the same information-theoretic pipeline can be applied to glutamate, GABA, and glycine receptor systems. This provides a consistent basis for comparing how different receptor kinetics influence MIR.

4.3 Glutamate Signaling via AMPA Receptors

Glutamate is the main excitatory neurotransmitter in the central nervous system, and AMPA receptors are among the key ionotropic receptors involved in fast synaptic transmission. In this section, the AMPA receptor is modeled as a ligand-dependent state-transition system, where glutamate concentration affects the transition rates between receptor states. The goal is to use this kinetic model to evaluate how changes in glutamate input concentration are reflected in the receptor-state output using MIR.

4.3.1 Receptor Background and Kinetic Scheme

Glutamate is the brain's principal excitatory neurotransmitter and plays a central role in fast synaptic communication and neuronal excitability. Glutamate receptors can be broadly divided into two main classes: ionotropic receptors, which are ligand-gated ion channels, and metabotropic receptors, which are G-protein-coupled receptors. The main ionotropic glutamate receptors are AMPA, NMDA, and kainate receptors, while the metabotropic family includes eight mGluRs (mGluR1-mGluR8) [3, 77]. Among these, AMPA receptors are especially suitable for our study because they mediate fast excitatory responses and can be represented using discrete kinetic states such as closed, open, and desensitized states [7]. This makes them compatible with the same Markov-based framework used in the previous chapter, where receptor kinetics are translated into a continuous-time Q-matrix and analyzed using mutual information and MIR. In this work, GluR1 and GluR4 AMPA receptor channels

are selected because the chosen kinetic study provides explicit transition rate constants for these two channel types, allowing direct construction of the Q-matrix and comparison of how different AMPA subunit models affect information transmission [3, 7].

In the AMPA receptor transition scheme, Figure 4.1, R denotes resting or closed non-conducting receptor states, O denotes open conducting states, and D denotes desensitized non-conducting states. The numbers in the resting states, R_0-R_4, indicate the number of glutamate molecules bound to the receptor. Channel opening is represented by O_2, O_3, and O_4, corresponding to open states with two, three, or four glutamates. The first desensitized row, D_1-D_4, represents desensitized states with one to four glutamates bound. The additional deeper desensitized states, written here as D_2^2, D_2^3, and D_2^4, represent a second level of desensitization beyond the initial desensitized states. In these non-conducting states, the receptor has two partially closed binding domains, while the superscript indicates the number of glutamate molecules bound. Thus, D_2^2, D_2^3, and D_2^4 correspond to receptors with two partial domains and two, three, and four bound glutamates, respectively [7].

Table 4.1 includes the rate constants used for the GluR1 and GluR4 AMPA receptor kinetic models. These parameters define the main transition rates for channel opening and closing, glutamate binding and unbinding, and entry into and recovery from desensitized states. The values are used to construct the corresponding transition-rate matrix for each receptor subtype and to support the subsequent MIR analysis.

Table 4.1: Rate constants for GluR1 and GluR4 channels, adapted from [7].

Parameter	**GluR1**	**GluR4**
α	3100 s^{-1}	8000 s^{-1}
β	8000 s^{-1}	20000 s^{-1}
k_1	2×10^7 $M^{-1}s^{-1}$	1×10^7 $M^{-1}s^{-1}$
k_{-1}	9000 s^{-1}	10000 s^{-1}
k_2	910 $M^{-1}s^{-1}$	1000 $M^{-1}s^{-1}$
k_{-2}	0.41 s^{-1}	1 s^{-1}
δ_0	3.3×10^{-3} s^{-1}	3.5×10^{-3} s^{-1}
γ_0	1 s^{-1}	6 s^{-1}
δ_1	1800 s^{-1}	800 s^{-1}
γ_1	7.6 s^{-1}	45 s^{-1}
δ_2	200 s^{-1}	4000 s^{-1}
γ_2	35 s^{-1}	220 s^{-1}

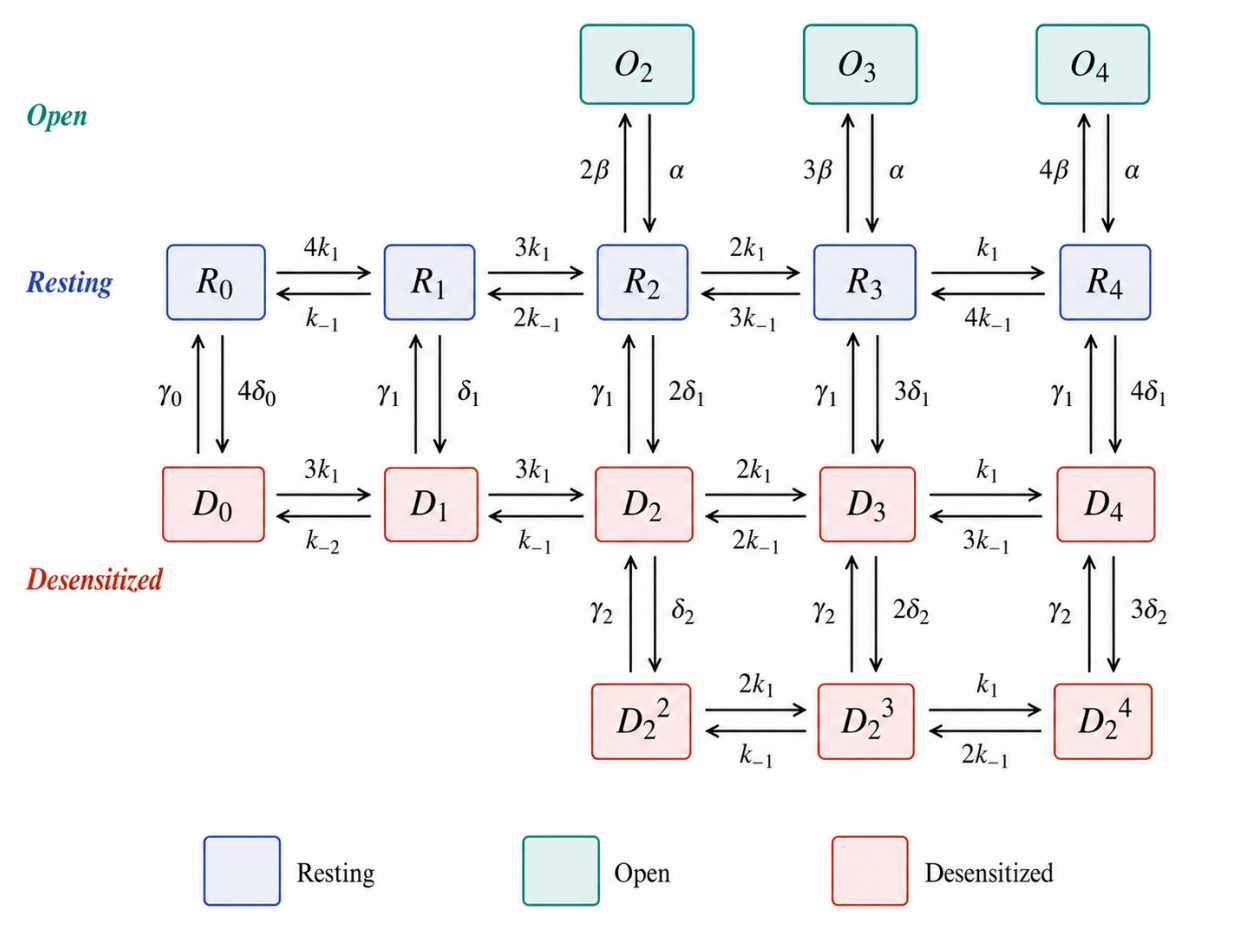

Figure 4.1: Kinetic transition scheme for the AMPA receptor, adapted from [7]. Low-probability gray states and transitions from the original model are excluded.

4.3.2 MIR Analysis

To evaluate the MIR of glutamate by AMPA receptor dynamics, we modeled GluR1 and GluR4 as continuous-time Markov chains using the kinetic scheme and rate constants reported by Robert and Howe [7]. For each receptor subtype, we constructed two generator matrices corresponding to a low glutamate concentration, x_L, and a high glutamate concentration, x_H. These matrices were then used to compute the MIR as a function of p_L, the probability of the low-concentration input. The concentration pairs were selected from the concentration-response results and experiments reported in [7]:

- Desensitization plateau: This case compares a low concentration that mainly reflects desensitization with a higher concentration associated with the plateau response. GluR1:

Table 4.2: Peak MIR across concentration regimes for GluR1 and GluR4 AMPA receptors. Concentrations are reported in μM and MIRs in bits/s.

Receptor	**Regime**	x_L	x_H	p_L^*	$MIR_{\max}$
GluR1	Desensitization plateau	0.56	12.5	0.6266	288.675
	Plateau peak	12.50	717.0	0.7427	9177.948
	Desensitization peak	0.56	717.0	0.7658	10735.505
	Experimental low-high	2.00	5000.0	0.8819	30665.821
	Experimental mid-high	50.00	5000.0	0.8609	26059.854
GluR4	Desensitization plateau	7.49	32.3	0.5976	173.472
	Plateau peak	32.30	1800.0	0.7417	10431.990
	Desensitization peak	7.49	1800.0	0.7578	11769.312
	Experimental low-high	8.00	5000.0	0.8288	22199.543
	Experimental mid-high	50.00	5000.0	0.8148	19962.442

[0.56–12.5 μM], GluR4: [7.49–32.3 μM].

- Plateau peak: This case compares the plateau-response range with the higher concentration range needed for the peak response. GluR1: [12.5–717 μM], GluR4: [32.3–1800 μM].

- Desensitization peak: This case captures the widest concentration-response range, from desensitization to peak activation. GluR1: [0.56–717 μM], GluR4: [7.49–1800 μM].

- Experimental low-high: This case follows the paper's low-concentration desensitization condition and compares it with the high test pulse. GluR1: [2 μM–5 mM], GluR4: [8 μM–5 mM].

- Experimental mid-high: This case compares an intermediate glutamate condition with the same high test pulse. GluR1: [50 μM–5 mM], GluR4: [50 μM–5 mM].

4.3.3 Results and Interpretation

The MIR results in Figure 4.2 show that the information rate depends strongly on the pair of glutamate concentrations being compared. In both GluR1 and GluR4, the lowest MIR is observed for the desensitization-plateau case, where the two concentrations are closer and

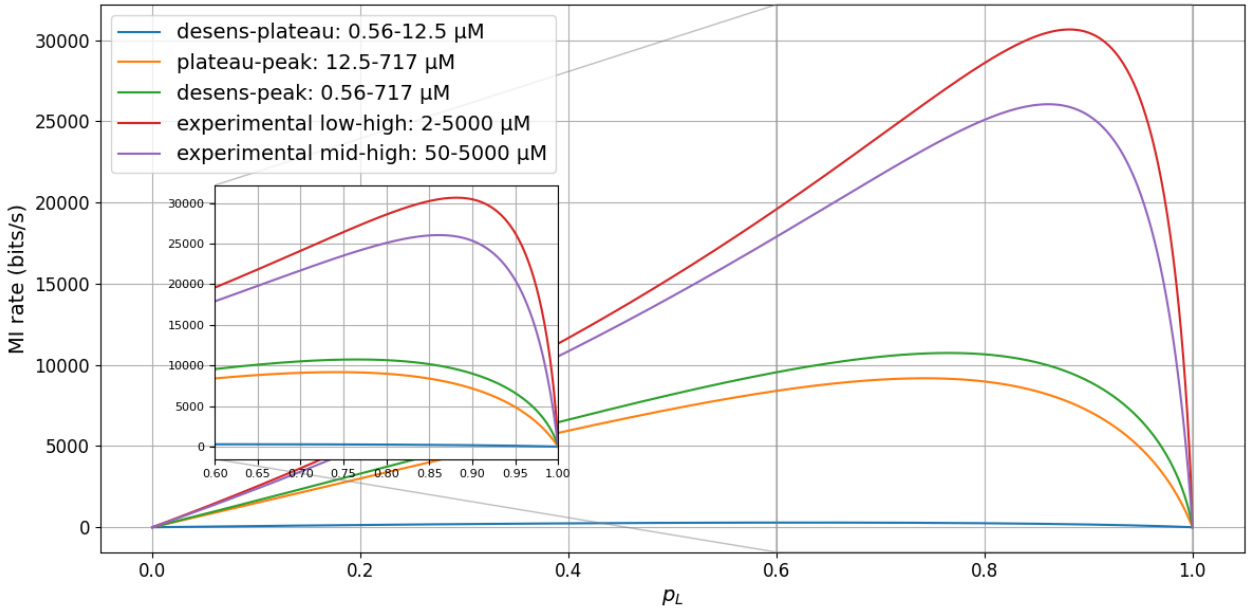

(a) GluR1

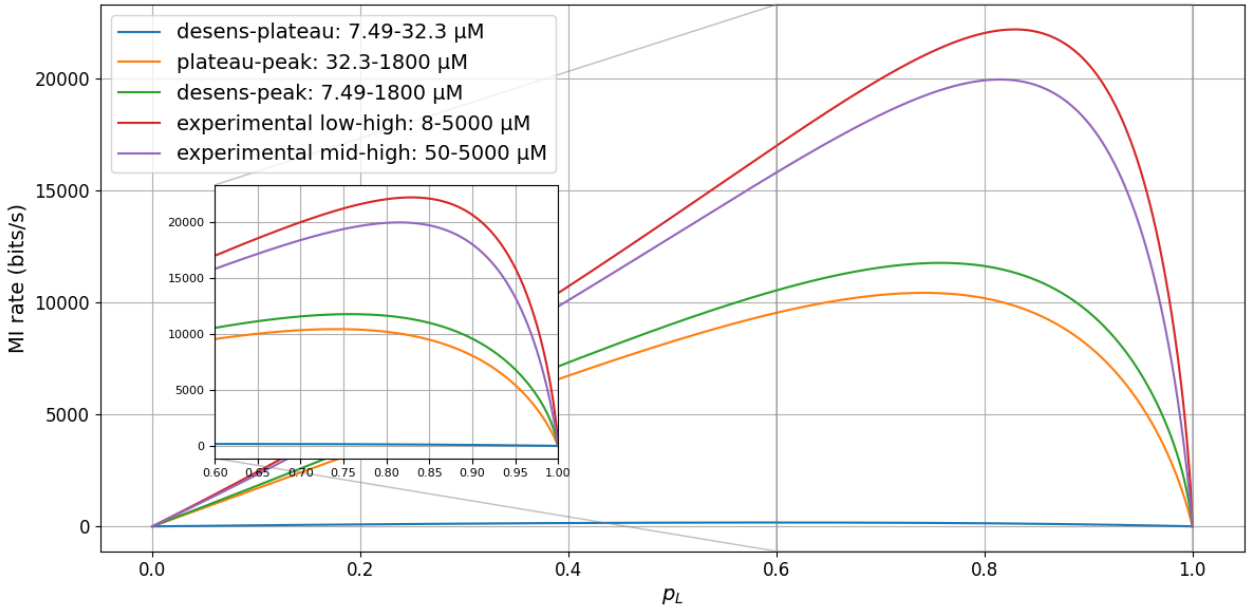

(b) GluR4

Figure 4.2: MIR as a function of p_L for (a) GluR1 and (b) GluR4 AMPA receptor models under different glutamate concentration ranges. Each curve compares a low concentration x_L with a high concentration x_H, using concentration pairs derived from the experimental results in [7].

both are within lower-response regimes. This suggests that the receptor-state dynamics are less distinguishable in this range.

Higher MIR values are observed for the plateau-peak, desensitization-peak, and experimental cases. These cases include a much larger separation between x_L and x_H, so the corresponding receptor dynamics are more different. This is consistent with the concentration-response results reported by Robert and Howe, where peak activation required much higher glutamate concentrations than desensitization or plateau current [7].

Biologically, this suggests that the AMPA receptor model carries more information when glutamate changes move the receptor between more distinct functional regimes, such as weak activation/desensitization and stronger activation at high glutamate. However, these MIR values should be interpreted as information in the simulated receptor-state dynamics, not directly as experimentally measured synaptic current. This distinction is important because only the open states contribute to conductance in the kinetic model, while closed and desensitized states are non-conducting. These results are summarized in Table 4.2.

4.4 GABA Signaling via $GABA_A$ Receptors

Gamma-aminobutyric acid (GABA) is the main inhibitory neurotransmitter in the mammalian central nervous system and plays a central role in reducing neuronal excitability [80]. In this work, GABA signaling is considered through $GABA_A$ receptors, which are ionotropic ligand-gated channels and are therefore suitable for state-based kinetic modeling. In computational terms, they can be represented as state-based systems in which ligand concentration drives transitions among closed, open, and desensitized receptor states, producing an inhibitory ionic current as the output. GABA also signals through $GABA_B$ receptors, which are metabotropic G-protein-coupled receptors rather than ion channels; therefore, they produce slower and more indirect signaling responses than $GABA_A$ receptors [80], and we will not be modeling in this chapter.

4.4.1 Receptor Background and Agonists

We consider three $GABA_A$ receptor subtypes: $\alpha_1\beta_3\gamma_2$, $\alpha_4\beta_3\gamma_2$, and $\alpha_4\beta_3\delta$. In biological terms, these labels describe the subunit composition of the receptor, or the specific protein components that form the receptor channel. The $\alpha_1\beta_3\gamma_2$ receptor is treated as a synaptic-type receptor, while $\alpha_4\beta_3\delta$ represents an extrasynaptic-type receptor; the $\alpha_4\beta_3\gamma_2$ receptor is

included as an intermediate comparison case. This distinction is important because synaptic receptors usually respond to brief, high-concentration GABA signals, whereas extrasynaptic receptors are more often exposed to lower but more persistent GABA levels. As a result, receptor subtype can affect ligand sensitivity, opening probability, desensitization, and the overall kinetic behavior used in the Markov model [8, 80, 81]. From a computational perspective, each subtype can be viewed as a different version of the same input-output system: the ligand provides the input, the receptor subtype defines the transition structure and rate constants, and the output is the resulting channel opening behavior.

In addition to the endogenous ligand GABA, meaning the natural ligand produced by the body, some kinetic studies also examine exogenous agonists such as muscimol and THIP [8]. Here, exogenous means that these ligands are produced from outside the biological system rather than naturally produced as the main neurotransmitter. These compounds are not separate neurotransmitters; rather, they are pharmacological agonists that bind to and activate $GABA_A$ receptors. In [8], GABA, muscimol, and THIP were compared across different $GABA_A$ receptor subtypes, including synaptic-type $\alpha_1\beta_3\gamma_2$ receptors and extrasynaptic-type $\alpha_4\beta_3\delta$ receptors. This is useful computationally because the ligands can be treated as different inputs, while the receptor subtype defines the state-transition system being tested.

4.4.2 Kinetic Scheme and Rate Constants

In Figure 4.3, the $GABA_A$ receptor is represented as a finite-state kinetic system in which the receptor moves between closed, open, and desensitized states. The symbol A represents the agonist, which can be GABA, muscimol, or THIP, and R represents the $GABA_A$ receptor in its unbound state. After one agonist molecule binds, the receptor enters the monoliganded closed state AR; after a second agonist molecule binds, it enters the biliganded closed state A_2R. From these ligand-bound closed states, the receptor can transition into conducting open states, denoted by AR^* and A_2R^*, where the asterisk indicates that the ion channel is open. The model also includes a desensitized state, A_2D, which is reached from the biliganded receptor state. This state is non-conducting, meaning the receptor is ligand-bound but temporarily unavailable for channel opening [8].

Table 4.3 includes the kinetic rate constants used to parameterize the $GABA_A$ receptor

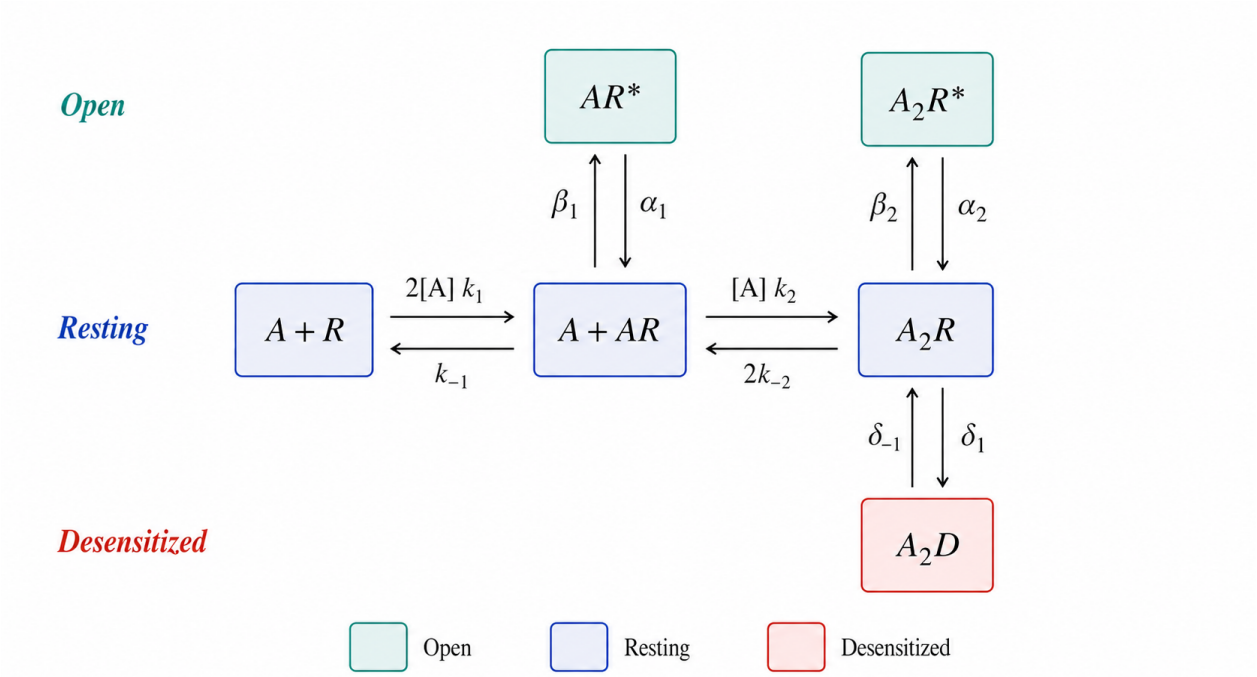

Figure 4.3: Kinetic transition scheme for $GABA_A$ receptor activation, adapted from [8]. The model includes agonist binding to resting closed states, transitions to mono-liganded and bi-liganded open states, and entry into a desensitized state. Here, A represents the agonist, R the receptor, AR^* and A_2R^* the open states, and A_2D the desensitized state.

Markov model for the three receptor subtypes and three agonists considered in [8]. These constants describe the transition rates between ligand binding and unbinding states, channel opening and closing states, and the desensitized state.

4.4.3 MIR Analysis

For readability purposes, we divide the MIR analysis of $GABA_A$ signaling into three parts, based on the agonist used to activate the receptor: GABA, muscimol, and THIP. In each part, the same three receptor subtypes, $\alpha_1\beta_3\gamma_2$, $\alpha_4\beta_3\gamma_2$, and $\alpha_4\beta_3\delta$, are compared using the experimentally selected concentration pairs from [8].

GABA as an endogenous agonist: For GABA, the selected concentration pairs were 0.3–3 μM, 3–30 μM, and 0.3–30 μM for the $\alpha_1\beta_3\gamma_2$ and $\alpha_4\beta_3\gamma_2$ receptors. For the $\alpha_4\beta_3\delta$ receptor, lower concentration pairs were used: 0.03–0.3 μM, 0.3–3 μM, and 0.03–3 μM. These pairs correspond to the low–mid, mid–high, and low–high input cases, respectively. Figure 4.4 shows the resulting MIR curves as a function of the low-concentration input probability p_L

Table 4.3: Kinetic rate constants for transitions between states of $\alpha_1\beta_3\gamma_2$, $\alpha_4\beta_3\gamma_2$, and $\alpha_4\beta_3\delta$ $GABA_A$ receptors activated by GABA, muscimol, and THIP. Values are adapted from Mortensen et al. [8].

Parameter	Unit	$\alpha_1\beta_3\gamma_2$			$\alpha_4\beta_3\gamma_2$			$\alpha_4\beta_3\delta$		
		GABA	Muscimol	THIP	GABA	Muscimol	THIP	GABA	Muscimol	THIP
k_1	$M^{-1}s^{-1}$	51×10^6	453×10^6	1.6×10^6	3.5×10^6	7.1×10^6	3.9×10^6	32×10^6	15×10^6	5.7×10^6
k_{-1}	s^{-1}	399	245	3	6	6	6	7	1.3	56
k_2	$M^{-1}s^{-1}$	28×10^6	186×10^6	2.6×10^6	3.2×10^6	5.9×10^6	0.8×10^6	47×10^6	21×10^6	0.15×10^6
k_{-2}	s^{-1}	360	428	842	51	28	285	12	7	53
δ	s^{-1}	219	217	110	2	5	6	6	6	7
δ_{-1}	s^{-1}	17	21	15	3	11	15	3	6	2
β_1	s^{-1}	570	427	40	57	45	39	20	22	142
α_1	s^{-1}	2268	2471	2695	2972	2887	1625	465	1324	956
β_2	s^{-1}	2556	2690	1543	936	887	676	255	325	1362
α_2	s^{-1}	356	324	394	970	1023	812	1500	1729	348

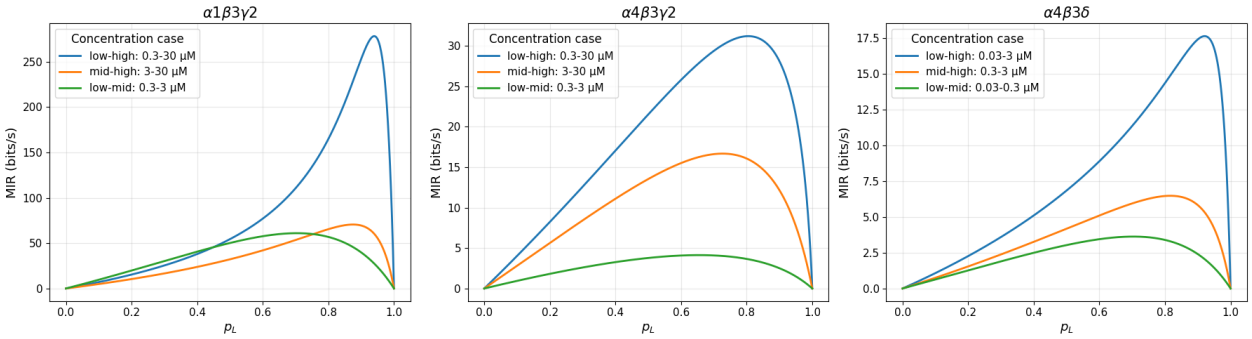

Figure 4.4: MIR analysis for GABA at three $GABA_A$ receptor subtypes. The three subplots compare $\alpha_1\beta_3\gamma_2$, $\alpha_4\beta_3\gamma_2$, and $\alpha_4\beta_3\delta$. Each curve shows one concentration-pair case: low–mid, mid–high, or low–high.

for the three receptor subtypes.

Muscimol as an exogenous agonist: For muscimol, the selected concentration pairs were 0.03–0.3 μM, 0.3–3 μM, and 0.03–3 μM for the low–mid, mid–high, and low–high cases, respectively. These same ranges were used for all three receptor subtypes. Figure 4.5 shows the corresponding MIR curves across p_L.

THIP as an exogenous agonist: For THIP, higher concentration ranges were used: 3–30 μM, 30–300 μM, and 3–300 μM for the low–mid, mid–high, and low–high cases, respectively. As with muscimol, these ranges were applied to all three receptor subtypes. Figure 4.6 summarizes the resulting MIR behavior across p_L.

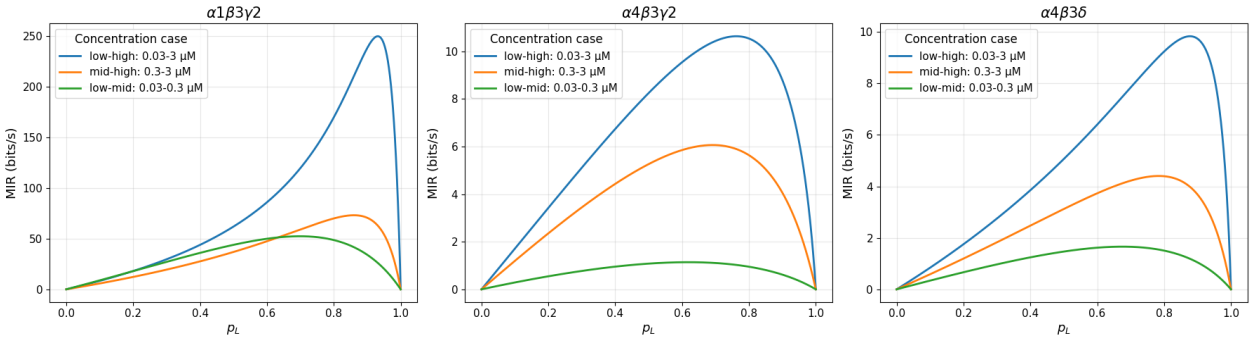

Figure 4.5: MIR curves for muscimol across the three $GABA_A$ receptor subtypes. Each subplot corresponds to one receptor subtype, and each curve represents one concentration-pair case.

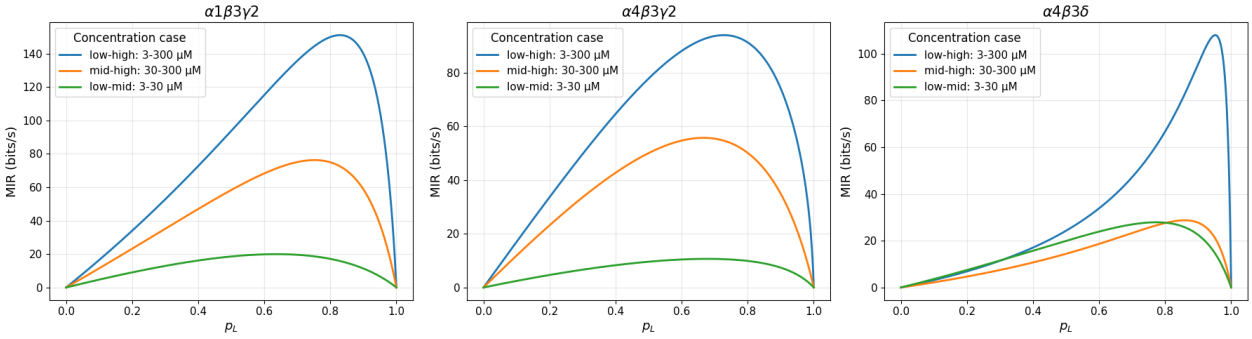

Figure 4.6: MIR curves for THIP across the three $GABA_A$ receptor subtypes. Each subplot corresponds to one receptor subtype, and each curve represents one concentration-pair case.

4.4.4 Results and Interpretation

Figure 4.7 compares the MIR curves of GABA, muscimol, and THIP under the low-high concentration case for the three $GABA_A$ receptor subtypes. The results show that the information-carrying behavior of the receptor models depends on both agonist identity and receptor subtype. For the $\alpha1\beta3\gamma2$ receptor, GABA and muscimol produced higher MIR values than THIP, with GABA reaching the highest value. In contrast, for the $\alpha4\beta3\gamma2$ and $\alpha4\beta3\delta$ receptors, THIP produced the strongest MIR response among the three agonists. This pattern is consistent with the experimental motivation for comparing GABA, muscimol, and THIP across synaptic- and extrasynaptic-type $GABA_A$ receptors, since receptor subunit composition can affect agonist-dependent activation properties [8]. Overall, these results suggest that MIR is not determined by concentration range alone, but by the interaction between agonist type and receptor-specific kinetic behavior.

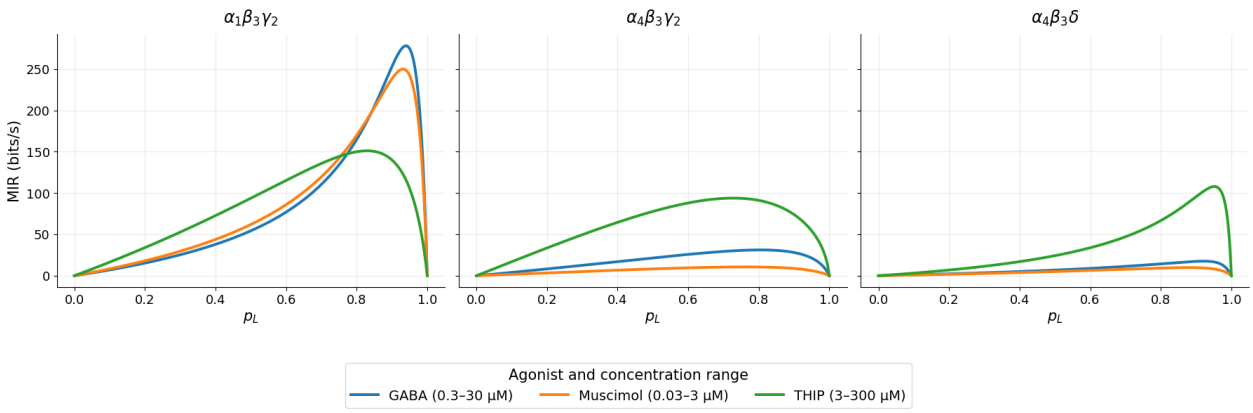

Figure 4.7: Comparison of MIR curves for GABA, muscimol, and THIP under the low-high concentration case. Each subplot shows one $GABA_A$ receptor subtype, and each curve represents the MIR as a function of the low-concentration input probability p_L.

Table 4.4: Peak MIR values for the low-high concentration case in Figure 4.7. Values are reported in bits/s.

Agonist	$\boldsymbol{\alpha 1\beta 3\gamma 2}$	$\boldsymbol{\alpha 4\beta 3\gamma 2}$	$\boldsymbol{\alpha 4\beta 3\delta}$
GABA	278.1	31.2	17.6
Muscimol	250.0	10.6	9.8
THIP	151.1	93.9	107.9

Table 4.4 summarizes the results for the low-high case.

4.5 Glycine Signaling via $\alpha_1\beta$ Receptors

Glycine is an inhibitory neurotransmitter whose main postsynaptic target is the glycine receptor (GlyR), an ionotropic receptor from the pentameric ligand-gated ion channel (pLGIC) family [5]. Unlike GABA, which can signal through both ionotropic $GABA_A$ receptors and metabotropic $GABA_B$ receptors (GPCRs), glycine does not have a known GPCR-type receptor; its fast signaling role is therefore mainly connected to the ligand-gated GlyRs [4]. In adult inhibitory synapses, GlyRs commonly contain $\alpha 1$ and β subunits, and this $\alpha 1\beta$ form is associated with faster responses than earlier developmental GlyR forms [4, 79]. From a modeling perspective, this makes the $\alpha 1\beta$ GlyR a suitable system for representing glycinergic signaling as an input-dependent ion-channel process, where glycine concentration modulates the probability of transitions among closed, intermediate or flipped, and open receptor states

[5, 9]. In the present analysis, this receptor is therefore treated as a stochastic biochemical communication channel whose output is determined by ligand-dependent state transitions.

4.5.1 Receptor Background and Kinetic Scheme

We consider $\alpha_1\beta$ glycine receptors because they are a major synaptic form of GlyR in the adult nervous system. In this receptor, glycine binding does not simply switch the channel from closed to open. Instead, the receptor passes through several ligand-bound states before reaching an open conducting state [9].

In Figure 4.8, A represents glycine, R represents the resting closed receptor, F represents a flipped but still closed receptor, and F^* represents the open conducting state. The receptor can bind up to three glycine molecules, producing states such as AR, A_2R, and A_3R, before moving into flipped states and then open states.

From a computational perspective, Figure 4.8 provides a finite-state Markov model in which glycine concentration controls transitions among resting, flipped, and open states. This makes it suitable for MIR analysis because the model separates ligand binding, pre-opening conformational change, and channel opening into distinct state transitions. The fitted rate constants reported in Table 4.5 are therefore used to construct the transition-rate matrix for the glycine receptor model.

4.5.2 MIR Analysis

In order to evaluate the MIR of the $\alpha 1\beta$ glycine receptor, the receptor is represented by resting closed states, flipped closed states, and open states. The input to the channel is the extracellular glycine concentration, while the output is defined by the receptor state. Therefore, the MIR was computed from the full concentration-dependent kinetic state sequence of Figure 4.8.

For the MIR analysis, we considered a binary input in which glycine switches between a low concentration x_L and a high concentration x_H. The probability of selecting the low concentration is denoted by p_L, while the probability of selecting the high concentration is $1 - p_L$. For each concentration case, the transition matrix was constructed from the concentration-dependent generator matrix, and the MIR was calculated as a function of p_L.

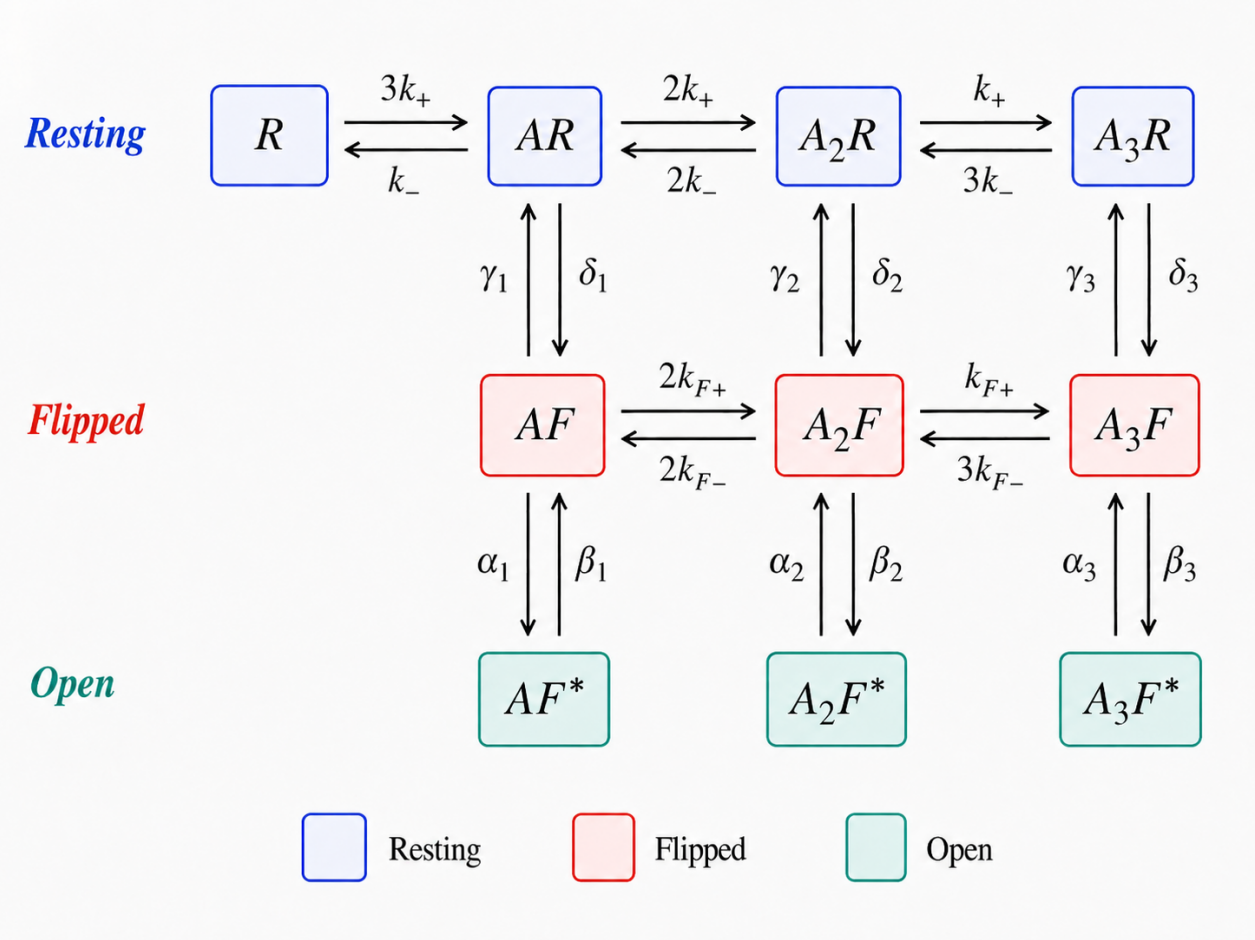

Figure 4.8: Flipped-state kinetic scheme for glycine receptor activation adapted from [9]. Resting (R) states are shown in blue, flipped (F) states in red, and open (F^*) states in green. Horizontal transitions describe glycine binding and unbinding, while vertical transitions describe conformational changes between resting, flipped, and open states.

This allowed us to compare how different glycine concentration ranges affect the amount of information that can be transmitted through the receptor.

For the glycine receptor analysis, we selected binary glycine input cases from the experimental range used in the original $\alpha1\beta$ GlyR single-channel study [9]. These cases were chosen to compare MIR under small, moderate, and wide concentration separations. We analyzed the $\alpha1\beta$ GlyR under the following binary glycine concentration cases:

- Low-mid: 10–100 μM
- Mid-high: 100–1000 μM
- Low-high: 10–1000 μM

Table 4.5: Kinetic rate constants for transitions scheme of the $\alpha_1\beta$ glycine receptor. Values are adapted from [9].

Parameter	Unit	$\alpha_1\beta$
α_1	s^{-1}	3400
β_1	s^{-1}	4200
α_2	s^{-1}	2100
β_2	s^{-1}	28000
α_3	s^{-1}	7000
β_3	s^{-1}	129000
γ_1	s^{-1}	29000
δ_1	s^{-1}	180
γ_2	s^{-1}	18000
δ_2	s^{-1}	6800
γ_3	s^{-1}	900
δ_3	s^{-1}	20900
k_-	s^{-1}	300
k_+	$M^{-1}s^{-1}$	0.59×10^6
k_{F-}	s^{-1}	1200
k_{F+}	$M^{-1}s^{-1}$	150×10^6

Table 4.6: Peak MIR summary for the $\alpha_1\beta$ glycine receptor across different glycine concentration regimes.

Case	x_L **(μM)**	x_H **(μM)**	**Peak** p_L	$MIR_{\max}$
Low–mid	10	100	0.5886	70.67
Mid–high	100	1000	0.8158	162.55
Low–high	10	1000	0.8999	462.62
P_{open} low–high	30	1000	0.8859	339.57
EC_{50}–high	60	1000	0.8569	236.41

- P_{open} low-high: 30–1000 μM
- EC_{50}-high: 60–1000 μM

These cases allow us to compare MIR across experimentally relevant low, intermediate, high, and near-EC_{50} glycine regimes.

4.5.3 Results and Interpretation

The largest MIR was observed for the low–high case (10–1000 μM), reaching 462.62 bits/s, because this input pair contrasts weak receptor activation with near-saturating activation.

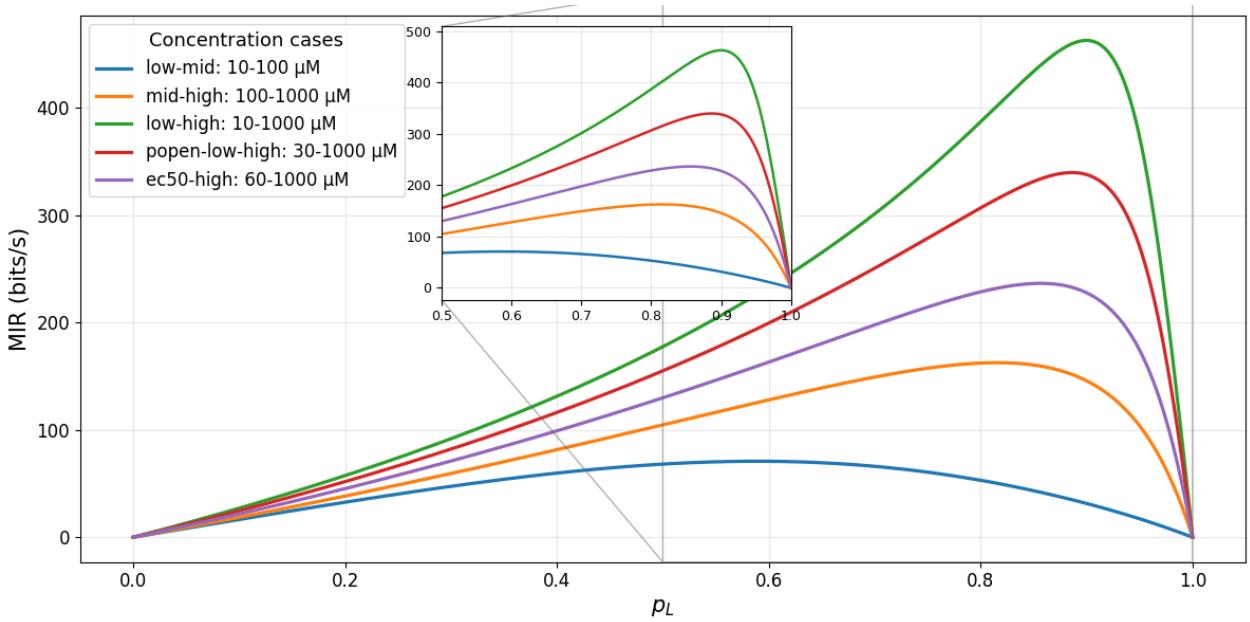

Figure 4.9: MIR analysis of the $\alpha 1\beta$ glycine receptor model. The curves show the MIR as a function of the low-concentration input probability p_L for a binary glycine input with concentration levels x_L and x_H.

Increasing the low concentration from 10 to 30, 60, and 100 μM progressively reduced the peak MIR, suggesting that the low input becomes less distinguishable from the high input as it enters the receptor's activation range. Therefore, the results indicate that MIR depends not only on the numerical distance between x_L and x_H, but on their functional separation in the receptor's kinetic state space. The high optimal p_L values further suggest that information transfer is maximized when low glycine is the dominant background condition and high glycine occurs as a less frequent, strongly informative signal.

4.6 Conclusion

This chapter extended the information-theoretic framework developed in the previous chapter to three other neurotransmitter systems: glutamate, GABA, and glycine signaling. Each system was represented using an ionotropic receptor model whose dynamics can be described through ligand-dependent transitions among discrete receptor states (such as closed, open, and desensitized states). This allowed the same continuous-time Markov modeling and MIR analysis to be applied across these receptor systems.

Across the three receptor systems, the results show that MIR depends strongly on how distinguishable x_L and x_H are. In general, concentration pairs that moved the receptor between more distinct functional regimes produced higher MIR values. Therefore, the relevant factor was not only the numerical separation between x_L and x_H, but also whether those concentrations produced meaningfully different probabilities of ligand binding, channel opening, or desensitization.

The results suggest that MIR often increases as the ratio x_H/x_L increases. However, this relationship is not strictly monotonic. Cases with the same ratio can produce different MIR values, and cases with smaller ratios can sometimes produce higher MIRs when the absolute concentration range lies in a more sensitive region of the receptor response. Therefore, x_H/x_L is a useful explanatory variable, but it is not sufficient by itself.

For the **AMPA** receptor models, both GluR1 and GluR4 showed the lowest MIR values in the desensitization plateau case, where the concentration levels were relatively close and belonged to lower response regimes. The MIR increased substantially when the concentration pair spanned a wider range. For example, the maximum MIR increased from 288.675 bits/s in the GluR1 desensitization plateau case to 30665.821 bits/s in the experimental low-high case. A similar pattern was observed for GluR4, where the maximum MIR increased from 173.472 bits/s to 22199.543 bits/s (Table 4.2). This indicates that the AMPA receptor models transmit more information when glutamate changes drive clearly different activation and desensitization dynamics. In this receptor model, the experimental mid-high case can produce a higher MIR than the desensitization peak case despite having a smaller x_H/x_L ratio. Thus the mid-high pair likely produces more distinct receptor-state dynamics within the selected kinetic model, especially through differences in ligand binding, channel opening, and desensitization. Therefore, the ratio x_H/x_L is a useful variable, but it is not sufficient to predict MIR by itself.

For the $\mathbf{GABA_A}$ receptor models, the results showed that MIR was shaped by both the agonist and the receptor subtype. In the $\alpha_1\beta_3\gamma_2$ receptor, GABA produced the highest low-high case MIR among the three agonists, reaching 278.142 bits/s, followed closely by muscimol at 249.987 bits/s, while THIP produced a lower value of 151.141 bits/s. However, this ordering changed for the $\alpha_4\beta_3\gamma_2$ and $\alpha_4\beta_3\delta$ receptors, where THIP produced the highest

low-high case MIR values. This suggests that information transmission in these receptor models is not determined by concentration range alone, but by the interaction between the agonist and the receptor subtype (Table 4.4). The ratio analysis supports this interpretation: the low-high cases generally produced the largest MIR values because they had the largest x_H/x_L ratios, but low-mid and mid-high comparisons with the same ratio often produced different MIRs. This shows that the absolute concentration range and receptor-specific kinetic sensitivity also affect the distinguishability of the receptor-state dynamics.

For the $\boldsymbol{\alpha_1\beta}$ **glycine** receptor model, the highest MIR was obtained in the low-high case, where 10 μM glycine was compared with 1000 μM glycine, reaching 462.62 bits/s. When the low concentration was increased from 10 μM to 30 μM, 60 μM, and 100 μM, the peak MIR decreased to 339.57, 236.41, and 162.55 bits/s, respectively. This pattern suggests that the low input becomes less distinguishable from the high input as it increases. Therefore, in this model, glycine signaling carries the most information when a low concentration background is contrasted with a less frequent high-concentration input (Table 4.6). The ratio analysis shows a similar but not complete trend: the largest ratio, $x_H/x_L = 100$, produced the highest MIR, but the low-mid and mid-high cases both had a ratio of 10 while producing different MIRs, showing that MIR is not determined by the ratio alone, but also by the absolute concentration range and how that range affects the receptor-state distribution.

Overall, this chapter demonstrates that MIR provides a common computational measure for comparing different ionotropic receptor models. The results show that receptor kinetics strongly influence how concentration changes are encoded in receptor-state dynamics. At the same time, the absolute MIR values should be interpreted carefully, because each receptor model has a different state structure, transition-rate scale, and biological role. Therefore, the main contribution of this chapter is not a direct physiological ranking of glutamate, GABA, and glycine signaling, but a model-based comparison showing how different receptor kinetics shape information transmission under controlled input conditions.

5 Conclusion

The main contribution of this thesis is a reusable computational framework for converting published receptor kinetic schemes into information-theoretic channel models and comparing their MIR under controlled input conditions.

In this work, we have investigated possible answers to the following question: **Can neurotransmitter receptor signaling be treated as an information channel, and what do MIR results reveal about various receptor systems?** To address this question, we studied neurotransmitter-receptor signaling from an information-theoretic and computational perspective. Specifically, we modeled receptor-level biochemical signaling as a stochastic communication process, where neurotransmitter concentration serves as the input signal and receptor-state dynamics form the channel response. The main goal was to quantify how effectively different receptor systems transmit information about changes in neurotransmitter concentration.

To do this, we used published kinetic receptor models and represented their state transitions through Markov-based channel models. Low and high neurotransmitter concentration levels were treated as binary inputs, and the resulting receptor-state dynamics were analyzed using MIR. We first applied this framework to serotonin and dopamine signaling at the human 5-HT3A receptor, then extended the same analysis to Glutamate AMPA receptors, $GABA_A$ receptors, and Glycine $\alpha_1\beta$ receptors. By comparing MIR across different concentration regimes, input probabilities, receptor subtypes, and agonists, this thesis connected biological receptor kinetics with quantitative measures of information transmission. This allowed receptor signaling efficiency to be compared across multiple neurotransmitter-receptor systems using a common information-theoretic framework.

5.1 Main Findings

The results of this thesis show that neurotransmitter-receptor signaling can be meaningfully analyzed as an information channel. Across the studied receptor systems, MIR provided a quantitative way to measure how much information receptor-state dynamics carry about neurotransmitter concentration. This supports the main idea of the thesis: receptor signaling

is not only a biochemical process, but can also be interpreted as a stochastic communication channel.

For serotonin and dopamine at the human 5-HT_{3A} receptor, the MIR results showed that information transmission depends strongly on receptor kinetics and not only on the difference between low and high concentration levels. In the serotonin case, increasing the concentration ratio improved MIR only up to an optimal range, after which the information rate decreased or became less sensitive to further increases. In contrast, dopamine showed a much larger MIR and reached a high information rate over a broader range of concentration ratios. These results suggest that the kinetic properties of the ligand-receptor interaction play a major role in determining how efficiently concentration changes can be distinguished.

The results also showed that the optimal input probability is not always balanced between low and high concentrations. When the concentration ratio increased, the MIR-maximizing input distribution shifted toward a higher probability of the low-concentration state. This means that, in most regimes we analyzed, information transmission is maximized when low concentration is common and high concentration occurs more rarely. Therefore, both the concentration values and their probability of occurrence affect the information carried by the receptor response.

Extending the framework to glutamate AMPA receptors, $GABA_A$ receptors, and glycine $\alpha_1\beta$ receptors showed that MIR does not follow a universal pattern across receptor systems. Instead, information transmission depends on the specific kinetic structure of each receptor model, including subtype composition, agonist-dependent transitions, and the degree to which low- and high-concentration inputs produce distinguishable receptor-state dynamics. AMPA receptors highlighted model-dependent differences in signaling efficiency, $GABA_A$ receptors showed the influence of subtype and agonist identity, and the glycine $\alpha_1\beta$ receptor emphasized the importance of clear dynamic separation between input levels. Overall, these results show that receptor-specific kinetics, rather than neurotransmitter identity alone, determine how efficiently concentration changes are transmitted.

Overall, the main finding is that MIR is shaped by a combination of concentration regime, input probability, receptor subtype, agonist identity, and kinetic transition structure. Across all models, larger concentration differences did not automatically guarantee higher infor-

mation transmission. Instead, the receptor must produce distinguishable state dynamics under different input concentrations. This makes MIR a useful measure for comparing neurotransmitter-receptor systems because it captures both the input concentration structure and the internal receptor kinetics.

5.2 Limitations and Future Directions

The framework developed in this thesis provides a useful starting point for studying neurotransmitter-receptor signaling as an information channel. Future work can build on this foundation by making the input model more realistic, expanding the range of receptor systems studied, and connecting the analysis more closely to experimental and data-driven approaches.

One direction is to move beyond the binary low and high concentration inputs used in this study. This binary setup made the MIR analysis easier to control and interpret, especially when comparing different receptor systems. However, neurotransmitter concentrations in biological environments vary continuously over time. Future studies could therefore use multi-level, continuous, or time-varying concentration signals to better represent synaptic dynamics and reduce the dependence of the results on a specific pair of concentration values.

Another direction is to revisit the analysis as more detailed kinetic models and experimental measurements become available. The MIR values reported in this thesis are based on published receptor-state models and their associated rate constants. These models provide a strong starting point, but different kinetic schemes or updated parameter values may lead to different information-theoretic results. Future work could compare alternative receptor models, include uncertainty in rate constants, and examine how sensitive MIR is to specific modeling assumptions.

The framework could also be extended to a wider range of receptor families and signaling mechanisms. In addition to studying more ionotropic receptor subtypes, future work could consider metabotropic receptors, such as GPCR-based dopamine and serotonin systems. These receptors involve slower intracellular cascades and more complex biochemical interactions, so they would require richer kinetic or dynamical models. Including them would give a broader picture of how different neurotransmitter systems transmit information.

Another useful extension is to study drug and agonist effects more systematically. In Sec-

tion 4, different agonists, such as THIP and muscimol, produced different MIR responses in $GABA_A$ receptor models. This suggests that ligand identity can affect not only the strength of a receptor response, but also the amount of information carried by receptor-state dynamics. Future pharmacological studies could use this type of analysis to compare endogenous neurotransmitters and drug-like compounds across receptor systems.

Finally, receptor-level MIR analysis could be connected to larger biological pathways and data-driven methods. This thesis focused mainly on receptor-state dynamics, which made it possible to study the role of receptor kinetics directly. A natural next step would be to include additional stages of synaptic signaling, such as neurotransmitter release, diffusion, postsynaptic current generation, and downstream cellular responses. Additionally, machine learning methods could be used to estimate or predict information-theoretic quantities from kinetic parameters, simulated traces, or experimental data.

5.3 Simplifications

To make the information-theoretic analysis computationally tractable and allow consistent comparison across receptor models, several simplifications are made throughout this thesis:

- **Binary concentration inputs:** Neurotransmitter concentration is represented by two discrete levels, x_L and x_H.
- **Receptor-level signaling:** The model begins at neurotransmitter concentration and ends at receptor-state dynamics. Processes such as neurotransmitter release and diffusion are not explicitly modeled.
- **Fixed kinetic parameters:** Published kinetic schemes and rate constants are used directly. Parameter uncertainty, biological variability, and changes in kinetic parameters across experimental or physiological conditions are not explicitly incorporated.
- **Simplified concentration dependence:** Ligand-binding transitions are assumed to scale with neurotransmitter concentration, while input-insensitive processes such as unbinding, gating, and desensitization are treated as concentration-independent.

- **Reduced kinetic schemes:** Transitions with unavailable kinetic rates or negligible contributions are omitted where appropriate.

- **Discrete numerical representation:** Continuous-time receptor dynamics are evaluated using transition matrices

$$P(x) = e^{Q(x)\Delta t},$$

with a fixed simulation time step of $\Delta t = 0.002$ ms.

Consequently, the reported MIR and capacity values should be interpreted as properties of the corresponding receptor-level kinetic models under controlled input assumptions, rather than as direct measurements of complete physiological neurotransmitter signaling.

5.4 Final Remarks

The main contribution of this thesis is the use of a common **information-theoretic framework** to compare multiple neurotransmitter-receptor systems. Instead of examining each receptor only in terms of biochemical activation or response strength, this work evaluated receptor behavior in terms of how much information its state dynamics carry about neurotransmitter concentration. This makes it possible to compare different receptor models using the same quantitative measure, even when they involve different neurotransmitters, agonists, receptor subtypes, and kinetic schemes.

Although the models used in this thesis are simplified and limited to receptor-level dynamics, they provide a useful starting point for studying neurotransmitter signaling efficiency in a more systematic way. The results suggest that receptor kinetics can be interpreted not only as biological mechanisms, but also as factors that shape information transfer. This perspective may support future work in computational neuroscience, molecular communication, and pharmacological modeling by showing how receptor dynamics can be analyzed through the lens of information transmission.

Bibliography

[1] David E Nichols and Charles D Nichols. Serotonin receptors. *Chemical reviews*, 108(5):1614–1641, 2008.

[2] Dale Purves, George J. Augustine, David Fitzpatrick, William C. Hall, Anthony-Samuel LaMantia, James O. McNamara, and Steven M. Williams, editors. *Neuroscience*. Sinauer Associates, Sunderland, MA, 3rd edition, 2004.

[3] Brian S Meldrum. Glutamate as a neurotransmitter in the brain: review of physiology and pathology. *The Journal of nutrition*, 130(4):1007S–1015S, 2000.

[4] NG Bowery and TG Smart. Gaba and glycine as neurotransmitters: a brief history. *British journal of pharmacology*, 147(S1):S109–S119, 2006.

[5] Ákos Nemecz, Marie S Prevost, Anaïs Menny, and Pierre-Jean Corringer. Emerging molecular mechanisms of signal transduction in pentameric ligand-gated ion channels. *Neuron*, 90(3):452–470, 2016.

[6] Ken Solt, Dirk Ruesch, Stuart A Forman, Paul A Davies, and Douglas E Raines. Differential effects of serotonin and dopamine on human 5-ht3a receptor kinetics: interpretation within an allosteric kinetic model. *Journal of Neuroscience*, 27(48):13151–13160, 2007.

[7] Antoine Robert and James R Howe. How ampa receptor desensitization depends on receptor occupancy. *Journal of Neuroscience*, 23(3):847–858, 2003.

[8] Martin Mortensen, Bjarke Ebert, Keith Wafford, and Trevor G Smart. Distinct activities of gaba agonists at synaptic-and extrasynaptic-type gabaa receptors. *The Journal of physiology*, 588(8):1251–1268, 2010.

[9] Valeria Burzomato, Marco Beato, Paul J Groot-Kormelink, David Colquhoun, and Lucia G Sivilotti. Single-channel behavior of heteromeric $\alpha 1\beta$ glycine receptors: an attempt to detect a conformational change before the channel opens. *Journal of Neuroscience*, 24(48):10924–10940, 2004.

[10] Andrew W Eckford and Peter J Thomas. The channel capacity of channelrhodopsin and other intensity-driven signal transduction receptors. *IEEE Transactions on Molecular, Biological, and Multi-Scale Communications*, 4(1):27–38, 2019.

[11] Kevin C Chen. Evidence on extracellular dopamine level in rat striatum: implications for the validity of quantitative microdialysis. *Journal of neurochemistry*, 92(1):46–58, 2005.

[12] Donita L Robinson, Andre Hermans, Andrew T Seipel, and R Mark Wightman. Monitoring rapid chemical communication in the brain. *Chemical reviews*, 108(7):2554–2584, 2008.

[13] Shuchang Zhao and Kiryl D Piatkevich. Techniques for in vivo serotonin detection in the brain: State of the art. *Journal of Neurochemistry*, 166(3):453–480, 2023.

[14] George J Augustine, David Fitzpatrick, William Hall, Anthony-Samuel Lamantia, Dale Purves, and Léonard White. *Neurosciences*. De Boeck Superieur, 2015.

[15] Michael J Caire, Vamsi Reddy, and Matthew Varacallo. Physiology, synapse. 2018.

[16] Thomas M Cover. *Elements of information theory*. John Wiley & Sons, 1999.

[17] Ryan Suderman, John A Bachman, Adam Smith, Peter K Sorger, and Eric J Deeds. Fundamental trade-offs between information flow in single cells and cellular populations. *Proceedings of the National Academy of Sciences*, 114(22):5755–5760, 2017.

[18] Nicholas M Timme and Christopher Lapish. A tutorial for information theory in neuroscience. *eneuro*, 5(3), 2018.

[19] Alex Rhee, Raymond Cheong, and Andre Levchenko. The application of information theory to biochemical signaling systems. *Physical biology*, 9(4):045011, 2012.

[20] Shinsuke Uda. Application of information theory in systems biology. *Biophysical reviews*, 12(2):377–384, 2020.

[21] Peter J Thomas and Andrew W Eckford. Capacity of a simple intercellular signal transduction channel. *IEEE Transactions on information Theory*, 62(12):7358–7382, 2016.

[22] Gavsper Tkavcik and Pieter Rein ten Wolde. Information processing in biochemical networks. *Annual review of biophysics*, 54, 2025.

[23] Gavsper Tkavcik and William Bialek. Information processing in living systems. *Annual Review of Condensed Matter Physics*, 7(1):89–117, 2016.

[24] Raymond Cheong, Alex Rhee, Chiaochun Joanne Wang, Ilya Nemenman, and Andre Levchenko. Information transduction capacity of noisy biochemical signaling networks. *science*, 334(6054):354–358, 2011.

[25] Artemy Kolchinsky and David H Wolpert. Semantic information, autonomous agency and non-equilibrium statistical physics. *Interface focus*, 8(6):20180041, 2018.

[26] Andrew W Eckford. The philosophy and science of biological information theory: A brief overview and recent results. In *International Zurich Seminar on Information and Communication (IZS 2026)*, pages 131–136. ETH Zurich, 2026.

[27] Toby Berger and William B Levy. A mathematical theory of energy efficient neural computation and communication. *IEEE Transactions on Information Theory*, 56(2):852–874, 2010.

[28] Keyvan Aghababaiyan, Vahid Shah-Mansouri, and Behrouz Maham. Axonal channel capacity in neuro-spike communication. *IEEE transactions on nanobioscience*, 17(1):78–87, 2018.

[29] Mladen Veletić, Pral Anders Floor, Youssef Chahibi, and Ilangko Balasingham. On the upper bound of the information capacity in neuronal synapses. *IEEE Transactions on Communications*, 64(12):5025–5036, 2016.

[30] Lav R Varshney, Per Jesper Sjöström, and Dmitri B Chklovskii. Optimal information storage in noisy synapses under resource constraints. *Neuron*, 52(3):409–423, 2006.

[31] Mark D McDonnell, Shiro Ikeda, and Jonathan H Manton. An introductory review of information theory in the context of computational neuroscience. *Biological cybernetics*, 105(1):55–70, 2011.

[32] Eren Balevi and Ozgur B Akan. A physical channel model for nanoscale neuro-spike communications. *IEEE Transactions on Communications*, 61(3):1178–1187, 2013.

[33] Takuya Isomura, Koji Sakai, Kiyoshi Kotani, and Yasuhiko Jimbo. Linking neuromodulated spike-timing dependent plasticity with the free-energy principle. *Neural computation*, 28(9):1859–1888, 2016.

[34] Alexander Borst and Frédéric E Theunissen. Information theory and neural coding. *Nature neuroscience*, 2(11):947–957, 1999.

[35] Mladen Veletić and Ilangko Balasingham. Synaptic communication engineering for future cognitive brain–machine interfaces. *Proceedings of the IEEE*, 107(7):1425–1441, 2019.

[36] Mladen Veletić and Ilangko Balasingham. An information theory of neuro-transmission in multiple-access synaptic channels. *IEEE Transactions on Communications*, 68(2):841–853, 2019.

[37] Myongin Oh and Donald F Weaver. Alzheimer's disease as a fundamental disease of information processing systems: An information theory perspective. *Frontiers in Neuroscience*, 17:1106623, 2023.

[38] Hanlin Xiao, Kamela Dokaj, and Ozgur B Akan. What really is "molecule" in molecular communications? the quest for physics of particle-based information carriers. *IEEE Transactions on Molecular, Biological, and Multi-Scale Communications*, 10(1):43–74, 2023.

[39] Rubén Herzog, Pedro AM Mediano, Fernando E Rosas, Paul Lodder, Robin Carhart-Harris, Yonatan Sanz Perl, Enzo Tagliazucchi, and Rodrigo Cofre. A whole-brain model of the neural entropy increase elicited by psychedelic drugs. *Scientific reports*, 13(1):6244, 2023.

[40] A Ezequiel Pereyra, Camilo J Mininni, and B Silvano Zanutto. Information capacity and robustness of encoding in the medial prefrontal cortex are modulated by the bioavailability of serotonin and the time elapsed from the cue during a reward-driven task. *Scientific Reports*, 11(1):13882, 2021.

[41] Mohammad Samavat, Thomas M Bartol, Kristen M Harris, and Terrence J Sejnowski. Synaptic information storage capacity measured with information theory. *Neural Computation*, 36(5):781–802, 2024.

[42] Anthony A Grace. The tonic/phasic model of dopamine system regulation and its implications for understanding alcohol and psychostimulant craving. *Addiction*, 95(8s2):119–128, 2000.

[43] Sanjeev Sharma, Dharmendra Dixit, and Kuntal Deka. Deep learning based symbol detection for molecular communications. In *2020 IEEE International Conference on Advanced Networks and Telecommunications Systems (ANTS)*, pages 1–6. IEEE, 2020.

[44] Ethungshan Shitiri, Akarsh Yadav, Sergi Abadal, Eduard Alarcón, and Ho-Shin Cho. Enhanced drug delivery via localization-enabled relaying in molecular communication nanonetworks. In *Proceedings of the 11th Annual ACM International Conference on Nanoscale Computing and Communication*, pages 21–27, 2024.

[45] Abhinav Goyal, Una Karanovic, Charles D Blaha, Kendall H Lee, Hojin Shin, and Yoonbae Oh. Toward precise modeling of dopamine release kinetics: Comparison and validation of kinetic models using voltammetry. *ACS omega*, 9(31):33563–33573, 2024.

[46] David Colquhoun and Alan G Hawkes. On the stochastic properties of bursts of single ion channel openings and of clusters of bursts. *Philosophical Transactions of the Royal Society of London. Series B, Biological Sciences*, pages 1–59, 1982.

[47] Xuan Chen, Fei Ji, Miaowen Wen, Yu Huang, and Andrew W Eckford. Mutual information rate of gaussian and truncated gaussian inputs on intensity-driven signal transduction channels. *IEEE Communications Letters*, 27(8):1989–1993, 2023.

[48] Alain Destexhe, Zachary F Mainen, Terrence J Sejnowski, et al. Kinetic models of synaptic transmission. *Methods in neuronal modeling*, 2:1–25, 1998.

[49] Jeremias Corradi, Fernanda Gumilar, and Cecilia Bouzat. Single-channel kinetic analysis for activation and desensitization of homomeric 5-ht3a receptors. *Biophysical journal*, 97(5):1335–1345, 2009.

[50] Uche AK Chude-Okonkwo, BT Maharaj, Athanasios V Vasilakos, and Reza Malekian. Information-theoretic model and analysis of molecular signaling in targeted drug delivery. *IEEE transactions on nanobioscience*, 19(2):270–284, 2020.

[51] Sebastian Lotter, Arman Ahmadzadeh, and Robert Schober. Synaptic channel modeling for dmc: Neurotransmitter uptake and spillover in the tripartite synapse. *IEEE Transactions on Communications*, 69(3):1462–1479, 2020.

[52] Zachary M Sheffler, Vamsi Reddy, and Leela Sharath Pillarisetty. Physiology, neurotransmitters. In *StatPearls [Internet]*. StatPearls Publishing, 2023.

[53] Annalisa Scimemi and Marco Beato. Determining the neurotransmitter concentration profile at active synapses. *Molecular neurobiology*, 40(3):289–306, 2009.

[54] Ivo Siekmann, Larry E Wagner, David Yule, Colin Fox, David Bryant, Edmund J Crampin, and James Sneyd. Mcmc estimation of markov models for ion channels. *Biophysical journal*, 100(8):1919–1929, 2011.

[55] William J Anderson. *Continuous-time Markov chains: An applications-oriented approach*. Springer Science & Business Media, 2012.

[56] Lawrence R Rabiner. A tutorial on hidden markov models and selected applications in speech recognition. *Proceedings of the IEEE*, 77(2):257–286, 1989.

[57] L Venkataramanan and FJ Sigworth. Applying hidden markov models to the analysis of single ion channel activity. *Biophysical journal*, 82(4):1930–1942, 2002.

[58] Jutta Walstab, Gudrun Rappold, and Beate Niesler. 5-ht3 receptors: role in disease and target of drugs. *Pharmacology & therapeutics*, 128(1):146–169, 2010.

[59] Andrew J Thompson and Sarah CR Lummis. The 5-ht3 receptor as a therapeutic target. *Expert opinion on therapeutic targets*, 11(4):527–540, 2007.

[60] Claude Elwood Shannon. A mathematical theory of communication. *The Bell system technical journal*, 27(3):379–423, 1948.

[61] Jean-Martin Beaulieu and Raul R Gainetdinov. The physiology, signaling, and pharmacology of dopamine receptors. *Pharmacological reviews*, 63(1):182–217, 2011.

[62] Nariman Farsad, H Birkan Yilmaz, Andrew Eckford, Chan-Byoung Chae, and Weisi Guo. A comprehensive survey of recent advancements in molecular communication. *IEEE Communications Surveys & Tutorials*, 18(3):1887–1919, 2016.

[63] Leif ER Simmatis, Emma E Russo, Yasemin Altug, Vijairam Murugathas, Josh Janevski, Donghun Oh, Queenny Chiu, Irene E Harmsen, and Nardin Samuel. Towards discovery and implementation of neurophysiologic biomarkers of alzheimer's disease using entropy methods. *Neuroscience*, 558:105–113, 2024.

[64] Alessia Cacciotti, Chiara Pappalettera, Francesca Miraglia, Paolo Maria Rossini, and Fabrizio Vecchio. Eeg entropy insights in the context of physiological aging and alzheimer's and parkinson's diseases: a comprehensive review. *GeroScience*, 46(6):5537–5557, 2024.

[65] William Bialek. *Biophysics: searching for principles*. Princeton University Press, 2012.

[66] Nicholas M Barnes and Trevor Sharp. A review of central 5-ht receptors and their function. *Neuropharmacology*, 38(8):1083–1152, 1999.

[67] Lucie Polovinkin, Ghérici Hassaine, Jonathan Perot, Emmanuelle Neumann, Anders A Jensen, Solène N Lefebvre, Pierre-Jean Corringer, Jacques Neyton, Christophe Chipot, Francois Dehez, et al. Conformational transitions of the serotonin 5-ht3 receptor. *Nature*, 563(7730):275–279, 2018.

[68] Wolfram Schultz. Predictive reward signal of dopamine neurons. *Journal of Neurophysiology*, 80(1):1–27, 1998.

[69] Jakob K Dreyer, Kjartan F Herrik, Rune W Berg, and Jorn D Hounsgaard. Influence of phasic and tonic dopamine release on receptor activation. *Journal of neuroscience*, 30(42):14273–14283, 2010.

[70] Angelo Keramidas and Joseph W Lynch. An outline of desensitization in pentameric ligand-gated ion channel receptors. *Cellular and Molecular Life Sciences*, 70(7):1241–1253, 2013.

[71] David Papke, Giovanni Gonzalez-Gutierrez, and Claudio Grosman. Desensitization of neurotransmitter-gated ion channels during high-frequency stimulation: a comparative study of cys-loop, ampa and purinergic receptors. *The Journal of physiology*, 589(7):1571–1585, 2011.

[72] Nikolaos G Sgourakis, Pantelis G Bagos, Panagiotis K Papasaikas, and Stavros J Hamodrakas. A method for the prediction of gpcrs coupling specificity to g-proteins using refined profile hidden markov models. *BMC bioinformatics*, 6(1):104, 2005.

[73] Kodangattil R Sreekumar, Youping Huang, Mark H Pausch, and Kamalakar Gulukota. Predicting gpcr–g-protein coupling using hidden markov models. *Bioinformatics*, 20(18):3490–3499, 2004.

[74] Juan Manuel Lopez-Correa, Caroline König, and Alfredo Vellido. Gpcr molecular dynamics forecasting using recurrent neural networks. *Scientific reports*, 13(1):20995, 2023.

[75] Albert J Kooistra, Stefan Mordalski, Gáspár Pándy-Szekeres, Mauricio Esguerra, Alibek Mamyrbekov, Christian Munk, György M KeserHu, and David E Gloriam. Gpcrdb in 2021: integrating gpcr sequence, structure and function. *Nucleic Acids Research*, 49(D1):D335–D343, 2021.

[76] Ismael Rodríguez-Espigares, Mariona Torrens-Fontanals, Johanna KS Tiemann, David Aranda-García, Juan Manuel Ramírez-Anguita, Tomasz Maciej Stepniewski, Nathalie Worp, Alejandro Varela-Rial, Adrián Morales-Pastor, Brian Medel-Lacruz, et al. Gpcrmd uncovers the dynamics of the 3d-gpcrome. *Nature Methods*, 17(8):777–787, 2020.

[77] Andreas Reiner and Joshua Levitz. Glutamatergic signaling in the central nervous system: ionotropic and metabotropic receptors in concert. *Neuron*, 98(6):1080–1098, 2018.

[78] Masahito Watanabe, Kentaro Maemura, Kiyoto Kanbara, Takumi Tamayama, and Hana Hayasaki. Gaba and gaba receptors in the central nervous system and other organs. *International review of cytology*, 213:1–47, 2002.

[79] P Legendre. The glycinergic inhibitory synapse. *Cellular and Molecular Life Sciences CMLS*, 58(5):760–793, 2001.

[80] Amr Ghit, Dina Assal, Ahmed S Al-Shami, and Diaa Eldin E Hussein. Gabaa receptors: structure, function, pharmacology, and related disorders. *Journal of Genetic Engineering and Biotechnology*, 19(1):123, 2021.

[81] Richard W Olsen and Werner Sieghart. Gabaa receptors: subtypes provide diversity of function and pharmacology. *Neuropharmacology*, 56(1):141–148, 2009.